

**THERMAL AND MECHANICAL PROPERTIES OF POLYMERS
FILLED WITH COPPER POWDER**

by

JONATHAN ANDREW MOLEFI (B.Sc. Honours)

Submitted in accordance with the requirements for the degree

MASTER OF SCIENCE (M.Sc.)

Department of Chemistry

Faculty of Natural and Agricultural Sciences

at the

UNIVERSITY OF THE FREE STATE (QWAQWA CAMPUS)

SUPERVISOR: PROFESSOR AS LUYT

February 2005

DECLARATION

I, the undersigned, hereby declare that the research in this thesis is my own original work, which has not partly or fully been submitted to any other University in order to obtain a degree.



Molefi JA (Mr)



Luyt AS (Prof)

DEDICATION

Ho bana ba thari e ntsho. Hlomelang ka thuto, hoba ntwana e a loana. Ho mesuwe le mesuwetsana yohle e mphahlollotseng mahlo thutong, setsong, dipolotiking le bononong peo ya lona ha e a wela majweng. Ena ke tshwelopele ya leeto....

ABSTRACT

The aim of this study was to prepare LDPE-Cu and LLDPE-Cu composites containing different amount of copper, and to determine the morphology, surface free energy, thermal and mechanical properties, as well as thermal and electrical conductivities of the samples. The copper powder particle distributions were found to be relatively uniform at both low and high copper contents. There was cluster formation of copper particles at higher Cu contents, as well as the formation of percolation paths of copper in the PE matrices. The surface free energy results show an increase in the total surface free energy and its disperse part, but a decrease in the polar part of the surface free energy for the Cu-PE composites in comparison with pure PE. There was an initial increase, followed by a decrease in melting temperature of LDPE with increasing copper content. When the observed enthalpy was compared with the expected enthalpy, a higher enthalpy was observed in the presence of low copper contents. For LLDPE the melting temperatures did not change appreciably. Comparison of the observed and expected enthalpies also showed that there was very little increase in total crystallinity. The TGA results show that there was a general decrease in thermal stability with increasing copper content in both LDPE and LLDPE. For LDPE the elongation and stress at break slightly decreased with increasing copper content, while the decrease in the case of LLDPE was much more significant. Young's moduli of LLDPE and its composites had slightly higher values than those of LDPE and its composites, because LLDPE is more crystalline and therefore more stiff than LDPE. These values strongly decreased from the values for both pure LDPE and LLDPE to those of their composites containing 2 vol.% copper, after which the moduli slightly increased with increasing copper content. The thermal conductivities of the composites were higher than that of the pure polyethylene matrix for both LDPE and LLDPE. A linear increase in thermal conductivity was observed with an increase in filler content. The electrical conductivity of polyethylene-copper composites increased with increasing copper content in the composite for both LDPE and LLDPE. From these results the percolation concentration was determined as 18.7 vol.% copper for both polymers.

TABLE OF CONTENTS

	Page
DECLARATION	ii
DEDICATION	iii
ABSTRACT	iv
TABLE OF CONTENTS	v
CHAPTER 1 (INTRODUCTION)	1
1.1 Background	1
1.2 Conductive polymer composites	3
1.3 Percolation theory	6
1.4 Electrical properties	9
1.5 Thermal properties	14
1.6 Mechanical properties	19
1.7 Surface energy	22
1.8 Polarized optical microscopy	23
1.9 Aim and scope of this work	24
CHAPTER 2 (EXPERIMENTAL)	25
2.1 Materials	25
2.1.1 Polyethylene	25
2.1.2 Copper powder	25
2.2 Methods	25
2.2.1 Preparation of composites	25
2.2.2 Differential scanning calorimetry (DSC)	26
2.2.3 Thermogravimetric analysis (TGA)	27
2.2.4 Tensile testing	27
2.2.5 Surface free energy testing	27
2.2.6 Electrical conductivity	27
2.2.7 Thermal conductivity	28
2.2.8 Polarized optical microscopy	28

CHAPTER 3 (RESULTS AND DISCUSSION)	29
3.1 Polarized optical microscopy	29
3.2 Surface free energy	29
3.3 Thermal properties	32
3.3.1 Differential scanning calorimetry (DSC)	32
3.3.2 Thermogravimetric analysis (TGA)	36
3.4 Mechanical properties	37
3.5 Thermal and electrical conductivity	43
CHAPTER 4 (CONCLUSIONS)	46
REFERENCES	48
ACKNOWLEDGEMENTS	53

CHAPTER ONE

INTRODUCTION

1.1 Background

The general tendency of man is to lead a comfortable life. For this he needs new and useful materials. The search for new materials has been going on for a long time. Many new materials have been developed in the 20th century. A composite is one such a material, which has revolutionized the concept of high strength.

A composite, as its name indicates, is made by combining two or more dissimilar materials in such a way that the resultant material has properties superior to any of its parental components. Unlike a chemical compound, the components of a composite neither take part in a chemical reaction nor dissolve completely in each other. They remain strongly bonded together while maintaining an interface between them, and they act in concert to give much improved performance.

Composites are not new materials. The first composite was probably made in Biblical times when man added chopped straw to clay to make stronger bricks. Steel rod reinforced concrete, widely used in modern buildings, is also an example of a composite. With the inexorable march of civilization, man felt that more novel materials are required. Necessity, as it is said, is the mother of invention. So, to meet his ever growing and diversifying needs, man started fabricating new materials from a judicious combination or manipulation of the old.

The tremendous progress in science and technology brought about the Industrial Revolution in the 19th century. As this revolution progressed and encompassed every aspect of human life, an increasing need was felt for materials capable of resisting fatigue, environmental corrosion, pressure, stress and exposure to chemicals. They also have to be adaptable for use under extreme temperature variations. Newer and more versatile materials in the form of composites evolved as an answer to this need.

Their emergence has an impact in several fields like transportation, marine engineering, chemical equipment and machinery, construction, electrical and electronic equipment, space technology, sports goods, and medical engineering. These alternatives to traditional materials took the industry by storm. Composites manufacturing is one of the

fastest growing industries, with the United States being the major consumer of these materials. The global consumption of composites is now around two million tons annually and is growing at a rate of ten percent every year [1].

Composites are materials based on the controlled distribution of one or more materials, termed as reinforcement, in a continuous phase of a second material, called the matrix. The reinforcement is added to provide strength and stiffness to a composite. The matrix is also known as 'binder' material. Its function is to make the composite resistant to degradation. The ultimate performance of a composite depends not only on the matrix and the reinforcement but also on the matrix-reinforcement interface. The interface is a critical part of composite technology [2]. A third material, called a coupling agent or compatibilizer, controls it. Alkyl silanes, organo titanates, high molecular weight carboxylic acids and esters are examples of coupling agents. These coupling agents have two different functional groups. One is attracted to the resin and the other to the surface of the filler [3]. However, when both the matrix and fibre are organic in nature, greater bonding is expected between these components and as a result a coupling agent is generally not required. The composite matrix can be a plastic (resin), a metal or a ceramic. It is responsible for the integrity of the composite compound. Plastic matrix based composites constitute more than 95 % of composite materials in use today. These may be either thermoplastics or thermosets. 95 % of the plastic matrices are thermoset in nature. Some of the thermoplastic matrix materials are polyethylene, polypropylene, and nylon. Unsaturated polyester, epoxy, and phenol-formaldehyde are examples of thermoset matrix materials [4].

In case of metal matrix composites, the choice of the metal is governed by factors such as light weight and high temperature resistance. The aerospace industry has always stressed its need for lightweight metals, metal alloys or substitutes, which could be used to make aircraft parts. These increase the fuel efficiency and maneuverability of an aircraft without jeopardizing safety. Boron reinforced aluminum is very popular for aircraft applications. Ceramic matrices are chosen for their toughness. A ceramic-ceramic composite is an exception to the normal definition of composites. In these composites, the ceramic matrix is reinforced with ceramic fibres. These are considered composites, even though both the matrix and reinforcement are ceramic, because the two are in different forms. The matrix may be a sheet or fluid and the reinforcement is in the fibre form [5].

The performance of a composite material not only depends on the selection of the matrix, reinforcing, and auxiliary materials, but also on the interface. The interface must be as narrow as possible. Sometimes the bonding between the matrix and the reinforcement may

be poor. In such cases the performance of the composite can be improved either by the modification of the reinforcement or the matrix [5].

1.2 Conductive polymer composites

Scientists have become more interested in creating conductive polymers. Common polymers are electrically insulating with volume resistivities ranging from 10^{12} to 10^{19} Ω .cm. There are two methods used to reduce polymer resistivities to 10^3 Ω .cm or less. One method involves the synthesis of intrinsically conductive macromolecules, which is made possible by adulteration of the polymer with small quantities of doping agents. The other approach is to add conductive fillers, such as copper or nickel powder, metal-coated glass spheres or fibres, to the resin [6].

The conductivity of a polymer composite, which contains dispersed conductive filler, depends on factors such as the size and shape of the filler particles, their spatial distribution within a polymer matrix, the interactions between the filler surface and the polymer matrix, and the contact resistance between adjacent particles [7, 8]. All these factors determine the conditions of charge transport from one particle to another, i.e., the conductivity of the filler phase. Taking into account all these factors gives a suitable processing method to obtain the composites and to improve the electrical characteristics of these systems. Contact resistance between the particles is important in the case where the filler volume concentration exceeds the percolation threshold and the charge transport through the filler phase takes place *via* direct contact between the particles. In this case, conductivity can be defined as metallic conductivity. On the other hand, when a thin, insulating polymer layer separates the filler particles, conductivity is dominated by charge transport *via* a tunneling effect [8].

Graphite is available in different sizes and shapes, and Nagata *et al.* [9] investigated the importance of these factors on conductivity. By modifying low-density polyethylene (LDPE) with both plate-like and spherical graphite, they found that the conductivity of LLDPE/graphite composites with spherical graphite particles increases with decreasing size, while the conductivity of composites with plate-like graphite particles increases linearly with increasing particle size.

Liu and Chung [10] studied the characteristics of conductivity-improved polypyrrole films *via* different procedures. In this study, three electrochemical procedures were used to improve the conductivity of polypyrrole (PPy) films. One is to modify PPy with valence copper. Another is to synthesize a polyethylene oxide (PEO)/PPy composite. The last is an

original method to polymerize PPy on a rough gold substrate pre-treated with an electrochemical oxidation-reduction cycle (ORC). They observed that electrical conductivity of PPy is attributed to the electrons hopping along and across the polymer chains with conjugating bonds, giving rise to more positively charged PPy, more available electron holes, longer polymer chains and more co-planar between interchains, are favorable for better conductivity. The PEO/PPy composite becomes more flexible and compact by incorporating PEO into the PPy matrix.

Thongruang *et al.* [11] investigated the correlated electrical conductivity and mechanical properties of high-density polyethylene filled with graphite (G) and carbon fibre (CF). Addition of CF to an HDPE/G composite was found to increase the conductivity relative to that of the HDPE/G composite at the same filler concentration. The observed increase in conductivity is more pronounced if the concentration of G is already above its threshold value. The conductivity of the composite was found to jump from $0.1 (\Omega \text{ cm})^{-1}$ at 50 wt % pure G, and from $\sim 5.0 (\Omega \text{ cm})^{-1}$ at 10 wt % pure CF to $\sim 18.0 (\Omega \text{ cm})^{-1}$ when these two fillers are combined in a 40/(50+10) (w/w) HDPE/(G+CF) composite. This result confirms that the conductivity of an HDPE/G composite, already loaded above its threshold concentration, can be significantly improved upon by addition of a reasonably small amount of CF.

Miyasaka *et al.* [12] reported that the conductivity of polyethylene/carbon black (PE/CB) composites jumps by 10 orders of magnitude at a critical concentration of CB, which they designate as the threshold concentration for CB, that is the percolation threshold [13, 14]. Graphite is another carbonaceous filler that has been incorporated into PE for electrical conductivity purposes [15]. Addition of G to thermoplastics generally combines the electrical properties of G with ease of processing, and may likewise promote attractive electrochemical, physical, mechanical and economical considerations [16].

Gu *et al.* [17] studied conductive polymer-modified boron-doped diamond (BDD) for DNA hybridization analysis. Taking advantage of the conducting nature of the BDD film, a thin layer of polyaniline/poly(acrylic acid) (PANI/PAA) composite polymer film could be readily electro-polymerized onto the diamond surface. The carboxylic acid residues in the polymer film act as the binding sites for DNA attachment, whilst the conductive polymer matrix enhances the electron-transfer between DNA and the diamond surface. Fluorescence microscopy and cyclic voltammetry measurements indicate that the polymer-modified BDD has minimal non-specific DNA adsorption, and provides a stable transduction platform for DNA sensing.

Zhao *et al.* [18] studied the conduction mechanism of carbon black (CB) filled poly(vinylidene fluoride) composites. The positive temperature coefficient (PTC) effect of CB filled poly(vinylidene fluoride) (PVDF) composites and the changes in resistivity under different conditions were studied. They found that there was some coherence between the volume expansion and the crystallite melting of PVDF. The homogenization diffusion of CB particles results in increasing resistivity during volume expansion and crystallite melting. At high temperature, the resistivity decrease is due to the agglomeration of CB particles or aggregates, which results in a new CB distribution of better conductivity. On basis of the experimental evidence, the volume expansion of the composite matrix, the diffusion of CB particles from the amorphous region to the melt crystalline region and the agglomeration of CB particles dominate the PTC effect of PVDF/CB composites.

Yu-chuan and Hwang [19] investigated the enhancement of conductivity stability of polypyrrole (PPy) films modified by valence copper and polyethylene oxide in an oxygen atmosphere. The results reveal that polymerization potential, solvents used in polymerization, modification of PPy with valence Cu, and introduction of polyethylene oxide (PEO) into PPy all significantly influence the conductivities of PPy films and their correspondent stabilities. Pure PPy, prepared in water at an over-oxidized potential, shows a serious decrease in conductivity. However, valence Cu-modified PPy and PEO-modified PPy can depress the ageing reaction, resulting in an electron transfer from Cu to the N⁺ of PPy and a more compact, dense surface and hydrogen bonds forming, respectively.

Feller *et al.* [20] investigated the influence of processing conditions on the sensitivity of conductive polymer composites to organic solvent vapours. The electrical properties of two conductive polymer composites (CPC) not yet studied in the literature, poly(amide12-b-tetramethylene oxide)-carbon black (PEBAX-CB) and poly(ethylene-co-ethyl acrylate)-carbon black (EEA-CB) in the presence of two organic solvent vapours, chloroform and toluene, have been studied as a function of processing conditions (in the melt by extrusion and from solution by casting). The experiments show that the electrical response of the CPC to solvent vapours can be modulated, not only by changing the chemical nature of the polymer, but also by tailoring the CPC morphology, i.e. the area accessible to solvent molecules both at a micro and nanometric scale. For this purpose, the use of block or statistical copolymers is interesting in achieving microphase separation or good CB dispersion, respectively. The results show on the one hand that important responses to solvent vapours $\Delta R/R_{\max}$ can be achieved with high conductivity samples, but at the detriment of response time. On the other hand, the use of the curve shape, i.e. the diffusion mode characterized by $\Delta R/R_{\max}$ versus \sqrt{t}

curves slope and onset, would allow them to decrease the number of CPC for vapor detection. Sorption kinetic measurements show that toluene diffusivity is about two times lower in EEA-CB than in EEA. This phenomenon can be explained by a barrier effect of the carbon black particles and a decrease of plasticization of EEA chains by toluene molecules due to interactions between EEA and CB. Therefore, the sensitivity of the CPC to solvent vapors results from conductive particles disconnection due to volume expansion during the matrix swelling.

Dilhan *et al.* [21] investigated the development of the electrical properties of composites as a function of the degree of mixedness of conductive filler into an insulating polymer. Increasing the time and hence, the specific energy input, during the mixing process results in a more homogeneous spatial distribution of conductive filler in the polymer matrix, which in turn results in a decrease of the volume conductivity of the composite. The decreasing conductivity of the composite is attributed to the better coating and hence the isolation of the conductive particles from each other, thus hindering the formation of a conductive network. Overall, these results suggest that the control of the electrical properties of a conductive composite could benefit from a good understanding and sufficient control of the dynamics of the mixing process and the resulting degree of mixedness of the conductive particles in the polymer matrix.

Yazici *et al.* [22] studied particulate-based conductive composites exploiting percolation-range microstructure. A tri-block copolymer with polystyrene end blocks and poly(ethylene-butylene) mid block was used as the primary matrix materials. Graphite powders with controlled particle size distributions were used as conductive fillers. Systematic studies were carried out varying the volume percent and mixing distribution characteristics of the filler particles. The volume resistivity of the composite exhibited a significant increase with the increased specific energy input. The increase was associated with the enhanced coating of conductive particles and better distribution of the matrix polymer as the specific energy input increased.

1.3 Percolation theory

The percolation theory was developed to mathematically deal with disordered media, in which the disorder is defined by a random variation in the degree of connectivity. The main concept of the percolation theory is the existence of a percolation threshold, defined in the following way: Suppose p is a parameter that defines the average degree of connectivity

between various sub-units of some arbitrary system. When $p = 0$, all sub-units are totally isolated from every other sub-unit. When $p = 1$, all sub-units are connected to some maximum number of neighboring sub-units. At this point, the system is connected from one side to the other, since there are paths that go completely across the system, linking one sub-unit to the next along the spanning cluster [23]. Now suppose, starting at $p = 1$, connections are randomly broken, so that p , the measure of average connectivity, decreases. The percolation threshold is the value of p , usually denoted p_c , at which there is no longer an unbroken path from one side of the system to the other. Alternately, if we start at $p = 0$, and randomly create connections, so that p increases, p_c is defined as the point at which a spanning cluster first appears. For p less than p_c , only isolated, non-spanning clusters can exist. For p greater than p_c , there is always a spanning cluster, although some isolated, non-spanning clusters can still be present.

Mamunya *et al.* [24] investigated the electrical and thermal conductivity of systems based on epoxy resin (ER) and poly(vinyl chloride) (PVC) filled with metal powder. Copper and nickel powder having different particle shapes were used as fillers. Their observations show that the electrical conductivity of the composites of ER and PVC containing copper were similar. For the ER-Ni systems, the percolation threshold was 0.085; while for the ER-Cu composites it was 0.050. The difference in the percolation threshold values for ER-Ni and ER-Cu relates to the influence of the particle shape on the filler packing density. In contrast to the electrical conductivity, the concentration dependence of the thermal conductivity shows no jump in the percolation threshold region. The shape and spatial distribution of dispersed filler particles are important factors controlling the electrical and thermal properties of metal-filled polymer systems.

When a polymer matrix having conductivity σ_p is filled with dispersed filler having a conductivity σ_f , the prepared composite gains a conductivity value σ . When the volume filler fraction ϕ reaches a critical value ϕ_c (so-called percolation threshold), an infinite cluster (IC) is formed, and the composite becomes conductive [25]. As the filler concentration increases from ϕ_c to the filling limit F , the value σ increases rapidly over several magnitudes, from the value of σ_c at the percolation threshold to a maximum value σ_m . Below the percolation threshold, the conductivity change is negligible and the conductivity of the composite is equal to the polymer conductivity σ_p or slightly higher.

One of the most important characteristics of the filler-polymer composites is the filler-packing factor (F) [26]. The value of F depends on the shape and on the possibility of the

skeleton or chained structure formation [27]. The parameter F is a limit of system filling and is equal to the highest possible filler volume fraction at a given type of packing factor:

$$F = V_f / (V_f + V_p) \quad (1)$$

where V_f is the volume occupied by the filler particle at the highest possible filler fraction and V_p the volume occupied by the polymer (space among filler particles). For statistically packed monodispersed spherical particles of any size, F is equal to 0.64 [28]. F decreases in the case of deviation of shape from spherical, as well as in the case of formation of the volume filler skeleton structure, due to increase of V_p . The use of polydispersed filler particles results in an increase of F . As a rule, real fillers have F values smaller than 0.64. Thus, the value of F characterizes the filler phase topology taking into account the shape, fraction size and spatial distribution of particles. Equation (2) links the value of F with the percolation volume of conductive sites, in the framework of the lattice model by Scher and Zallen [29]

$$\varphi_c = X_c F \quad (2)$$

where X_c is a critical parameter, which has the meaning of a site percolation probability. For any lattice type, X_c and F have such values, that their product percolation threshold equals approximately 0.16. Equation (2) is valid also in the case of randomly distributed conductive sites [30]. The model by Scher and Zallen predicts an insulator-conductor transition at a strict value of the critical volume of conductive sites. In real two-phase systems, a sharp conductivity increase occurs within the concentration region called the smearing region [31].

Equation (2) does not hold true when polymer-conductive phase interactions exist. In this case, the filler phase topology depends not only on the filler phase geometry but also on the interfacial interaction at the polymer-filler boundary. Consequently, the equation linking percolation threshold and packing factor F has a more complex nature [32]. According to Wessling's thermodynamic model, in this case the relationship between percolation threshold and packing factor is not defined by a constant, but includes parameters, which reflect the interaction between phases 1 (polymer) and 2 (filler) [33]. The formation of a dispersed filler segregated structure in the polymer matrix, may be achieved by pressing the mixture of thermoplastic polymer powder having particle size D and of conductive filler having particle size d , provided that $D \gg d$ [34, 35], extrusion or casting of a mixture of incompatible polymers provided that only one polymer contains conductive filler [36, 37], or filling the

polymer matrix with conductive and non-conductive fillers simultaneously, having particle sizes d and d_1 respectively, with $d_1 > d$. The segregated structure formation allows control of those properties susceptible to spatial filler particle distribution (electrical and thermal conductivity, dielectric and magnetic properties).

Feller *et al.* [38] comparatively studied the mechanical and electrical properties of conductive polymer composites of poly(ester) – short carbon fibres and poly(epoxy) – short carbon fibres. The reinforcement effect of SCF filled thermoset CPC is more important with the poly(epoxy) than with the poly(ester) matrix. Electrical measurements show a small amplitude positive temperature coefficient (PTC) effect between 90 and 160 °C. The percolation threshold is reached at about 1 % v/v SCF and higher conductivity is obtained with the poly(ester) matrix. Up to 3 % v/v, a good correlation between resistivity and relative Young's modulus is found.

Novák *et al.* [39] investigated the electrical conductivity and elongation at break of epoxy filled with electroconductive carbon black, graphite, or silver-coated basalt particles or fibres. Percolation concentrations were determined to be 14 vol. % for epoxy/carbon black composites, 22 vol. % for epoxy/graphite composites, 28-29 % for both epoxy/silver-coated basalt particles and fibres. The steepest increase in electrical conductivity and the most pronounced decrease in elongation at break occurred at a similar filler concentration range for all investigated systems.

Novák *et al.* [40] also investigated the correlation between electrical conductivity and elongation at break of polyurethane (PU) filled with two different grades of graphite, Ag-coated basalt particles and fibres. Percolation concentrations were determined to be approximately 21-22 vol. % for PU/graphite composites, 29 vol. % for both PU/Ag-coated particles and PU/Ag-coated fibers composites. The results show the same behaviour as in [39].

1.4 Electrical properties

Yang and Schruben [41] investigated the electrical resistivity behaviour of mold-cast metal filled polymer composites. Mold-cast metal filled composites made of poly(methyl methacrylate) and aluminum or nickel exhibited electrical resistance qualitative behaviour as predicted by the percolation and tunneling mechanisms. A precipitous change in resistivity of about 10^4 ohm.cm was found at volume concentrations of filler in the range of 18.5 to 19.8 volume percent. When comparing the non-filled polymer to the filled polymers, they observed

that certain of the samples' mechanical properties, such as strength, decreased significantly. They found that the aluminum-nickel composite conformed to the percolation-tunneling model for a well-dispersed system. Nickel has a lower resistance than aluminum, so their metal-filled composites had lower resistance. After adding metallic powder filler to the polymer, the material's physical properties decreased and its metal-like properties increased.

Dang *et al.* [42] investigated the dependence of dielectric behaviour on the physical properties of fillers (carbon fiber (CF), copper (Cu) and nickel (Ni) powders) in polymer-matrix composites. Low-density polyethylene (LDPE) – electrical conducting fillers were prepared *via* simple blending and hot-molding techniques. At the same concentration of the fillers, the dielectric constants of the composites with CF fillers were lower than those of the composites with Cu and Ni fillers, respectively. For these composites the dielectric loss decreases first and then increases with the experimental frequency. There was a higher dielectric loss in the composites loading Cu filler of 0.20 in the frequency areas from 10^4 to 10^7 Hz, which can be understood due to a large electrical conducting loss in the Cu-containing composite. The dielectric losses increase gradually with a rise of the volume fraction of Cu fillers, and the composites with CF and Ni fillers have the same dielectric loss values at the same concentration. The ac conductivity of the composites increases with increasing frequency and volume fraction of fillers. The conductivity of Cu is the biggest among three conductive fillers. Therefore, the conductivity of the composites with Cu fillers increases rapidly when the concentration of filler increases. It is assumed that an electrical conducting path and network could be formed in the composites with increasing the concentration of fillers [43, 44].

Kalyon and Birinci [45] investigated the electrical conductivity of a graphite-based composite as affected by the degree of mixedness of graphite in an elastomeric matrix. A wide-angle x-ray diffraction (WAXD) based quantitative phase analysis method was used. They observed that increasing the specific energy input during the mixing process resulted in a more homogeneous spatial distribution of graphite in the elastomer, and altered the rheology of the composite suggesting that significant structural changes did occur. The results show that volume resistivity of the composite increases exponentially with increasing the mixing time. The volume resistivity increases from $10^6 \Omega \text{ cm}$ at specific a energy input of 12 MJ kg^{-1} to $10^{11} \Omega \text{ cm}$ at specific energy input of 3.5 MJ kg^{-1} . Upon increasing the mixing time and hence the specific energy input incorporated during the mixing process, the homogeneity of the spatial distribution of the conductive graphite particles in the binder was improved and the conductive particles were better coated with the binder.

Biggs and Bhattacharya [46, 47] reviewed the development of the electrical properties of metal-filled polymers and the mechanism involved in the formation of conductive composites of polymer/metal systems. They found that metallic powders generally suffer from the oxidation of the metallic particles and the corresponding deterioration of the electrical properties of composites due to the non-conductive nature of such an oxide layer. The electrical properties of the composite are dependent on the concentration, size and shape distributions of the conductive particles [48, 49]. A number of studies revealed that the mixing time of the conductive filler into the polymer matrix also affects the ultimate electrical conductivity of the composite [50, 51].

Mamunya *et al.* [52] studied the influence of pressure on the electrical conductivity of metal powder used as fillers in polymer composites. They studied the influence of the particle size on the conductivity of the powders, and compared their data with that of the conductivity of composites based on an epoxy resin with the same metal powders as fillers. The results show that the dependence of electrical resistance on the powder thickness, for all size fractions of the copper powder, is linear. For the same value of the copper powder thickness, the measured resistance of the copper particles, having small size fraction, is higher than that of the bigger ones. For copper powder, the packing factor increased with increasing particle size, because small particles have more irregular shapes than the larger ones. Packing factors also increased with an increase in the applied pressure, due to the deformation of the particles. This change of the packing factor is affected by the hardness and size of the metal particles. Small copper particles deform more than larger ones.

Das *et al.* [53] investigated the effect of processing parameters, applied pressure and temperature on the electric resistivity of rubber-based conductive composites. Carbon black- and short carbon fibre (SCF)-filled conductive composites were prepared from ethylene vinyl acetate (EVA), ethylene propylene diene (EPDM) rubber and their 50:50 blends. The electrical resistivities of carbon black- and SCF-filled composites were measured under the different conditions. The electrical conductivity of filled polymer composites is due to the formation of a continuous conductive network in the polymer matrix [54]. This conductive network involves a specific spatial arrangement of conductive elements so that low resistance electrical paths are formed for free movement of electrons. It was found that electrical conductivity of filled conductive composites depends on different processing parameters, like mixing time, rotor speed, mixing temperature, vulcanization time and pressure, and service conditions like applied pressure and temperature. The results show that the electrical resistance of fibre is lower than the resistance of carbon black aggregates and this accounts for

high conductivities of the fibre-filled composites. The effect of mixing time on the volume resistivity of carbon- and SCF-filled composites initially show that the volume resistivity decreases with increasing mixing time in the case of carbon black-filled composites, and shows the lowest value within 2-3 min of mixing time. The volume resistivity increases rapidly with increasing mixing time. Slow decrease in resistivity at the beginning of the mixing is due to the formation of a conductive network by the distribution of the particulate black filler in the polymer matrix. A marginal change in resistivity is exhibited with further increase in mixing time. A different effect is observed in the case of carbon fibre-filled composites. Between 4 and 7 min of mixing there is only a marginal increase in resistivity, but beyond that the increase in resistivity with mixing time is much faster. Mixing causes breakdown of the carbon black structure and generally loose agglomerates, so-called secondary structures, break more easily, whereas the primary carbon structures in the form of particles and aggregates are relatively more stable towards mechanical shear.

The situation for SCF-filled composites is somewhat different. SCF is considered as a rigid brittle long chain of carbon aggregates, which undergoes extensive breakage during mixing with rubber [55, 56]. The increased mixing time reduces the aspect ratio (L/D), due to a reduction of carbon fibre length, while its diameter remains unchanged during mixing. Investigation of the effect of rotor speed on the volume resistivity of carbon black- and SCF-filled conductive composites showed that the resistivity increases at a faster rate with increase in rotor speed from 20 to 60 rev. min⁻¹ at fixed mixing time and temperature for carbon black-filled composites, but with further increase in rotor speed the rate of increase is relatively low. With increasing rotor speed, the carbon black aggregates are subjected to more shearing action leading to appreciable structure breakdown due to their frequent passage through shearing zones. The conductive network breakage takes place with increasing rotor speed, and hence the resistivity of the composite increases.

Investigation of the mixing temperature on the resistivity of the composites shows that with increasing mixing temperature the resistivity gradually decreases for both systems. The increase in mixing temperature reduces the viscosity of the matrix in the internal mixer, as a result of which the carbon particle aggregates and carbon fibres experience a lesser degree of shear during mixing. Thus the efficiency of black structure breakdown and fibre length reduction both decrease with an increase in mixing temperature. As a result, increase in mixing temperature acts favorably in the formation of a conductive network.

Tzeng and Chang [57] investigated the electromagnetic interference (EMI) shielding effectiveness of metal-coated carbon fibre-reinforced ABS composites. The coaxial

transmission line method was used to measure the EMI shielding effectiveness of the metal-coated carbon fibres-ABS composites. The carbon fibres were coated with copper or nickel using cementation and electroless deposition techniques. Copper-coated carbon fibres-ABS composites showed poor EMI shielding effectiveness due to a shorter fibre length distribution after composite fabrication. Among the metal-coated carbon fibres-ABS composites studied in this investigation, electroless nickel-coated carbon fibres-ABS composites showed the best EMI shielding capability. In spite of the lower electrical conductivity of electroless Ni-P coating compared with that of cementation nickel, EMI shielding effectiveness of the electroless nickel-coated carbon fibres-ABS composites is better due to excellent bonding between the electroless nickel coating and the fibres. The bonding between metal coating and the fibres is not satisfactory when the cementation method was used to deposit a metal layer. As a result, the metal coating tended to detach during the compounding process, and consequently, poor EMI shielding effectiveness was obtained for their composites.

Philip *et al.* [58] investigated the friction and wear of an electrically conductive polyester-carbon film. This behaviour was examined during dry reciprocating sliding against typical noble and base metal pins. While the frictional force was monitored continuously, the wear volume was determined at the conclusion of each test. The experimental results suggest that the carbon filler acted as an effective solid lubricant during tests against the noble metal pins. During tests against the base metal pins, at relative humidities above about 40 %, this lubricating mechanism was impaired, thus resulting in an increase in the friction and wear of the polyester-carbon composite. An adhesive wear mechanism is proposed to account for the observed behaviour.

Vilčáková *et al.* [59] investigated the switching effect in pressure deformation of silicone rubber-polypyrrole composites. Conductive silicone rubber-polypyrrole composites were prepared by cast molding of the polymer matrix components and chemically synthesized polypyrrole (PPy). Composites contained from 2.2 to 8.5 vol % of PPy. A sigmoid dependence of the conductivity of the original uncompressed sample on the filler was found and a PPy percolation threshold concentration lower than 4 vol % was estimated. Electrical conductivity of silicone rubber-polypyrrole composites in pressure deformation showed a steep decrease more than five orders of magnitude to values corresponding to an insulator. This "switching effect" had a good reproducibility, which suggests a possible use of this material in microelectronics.

1.5 Thermal properties

Kuljanin *et al.* [60] studied the influence of CdS filler particles in the micrometer size range on the properties of a polystyrene (PS) matrix, using structural and thermal techniques. An improvement of 50 K was found in the thermal stability of the PS matrix in the presence of CdS-filler. Infrared measurements revealed that the interaction between the surface of the CdS-filler particles and the PS chains was weak, and a possible reason for the increase in thermal stability was the partially altered molecular mobility of the polymer chains due to their adsorption on the surface of the CdS filler particles.

Weidenfeller *et al.* [61] investigated the thermal properties of injection-molded polypropylene samples with various fillers and filler fractions. As filler materials, copper, talc, magnetite, strontium ferrite, barite and glass fibers were selected to vary over a broad range of different filler properties, ranging from 2.58 (glass fibers) to 8.94 g/cm³ (copper) in density, and from nearly 1.5 (glass fibers) to approximately 400 W m⁻¹ K⁻¹ (copper) in thermal conductivity. The highest thermal conductivity of a composite was achieved with talc which has a moderate thermal conductivity ($\lambda_{\text{talc}} \approx 10.6 \text{ W m}^{-1} \text{ K}^{-1}$) compared to the high thermal conductivity of copper ($\lambda_{\text{copper}} \approx 400 \text{ W m}^{-1} \text{ K}^{-1}$). The thermal conductivity of the talc-filled polymer was increased from 0.27 to 2.50 W m⁻¹ K⁻¹ with 30 vol. % talc filler. This behaviour was a consequence of the microstructure of talc-filled PP showing a high interconnectivity of the talc crystals. The thermal conductivity of copper-filled polypropylene is, in spite of the very high conductivity of pure copper, lower than that of talc-filled PP composites due to the poor interconnectivity of the copper particles. To increase the thermal conductivity significantly without increasing the density very much, talc-filled composites seem to be a good candidate and can help to save cooling time during the injection molding process.

Araujo and Rosenberg [62] investigated the thermal conductivity of composites made from the epoxy resin Epikote 828 with metal powder fillers. The metals were Cu, Ag, Au, Al, Sn, Pb, stainless steel and bronze. In each case the thermal conductivity decreased monotonically as the temperature was reduced, but at higher temperatures it was substantially higher than that of the resin, especially for large volume concentrations of filler. At low temperatures, the effect of adding filler is very much reduced and is dependent on the particle size. In liquid helium range the conductivity of the samples containing 11 μm Cu and 10 μm Sn powders were lower than that of the unfilled resin. At higher temperatures, the thermal conductivity of the composite is dependent on the filler concentration and not on the filler material.

Kim *et al.* [63] studied the effect of temperature on the electrical resistivity and thermal conductivity of tungsten-copper (W-Cu) composites. W-Cu composites are promising materials for micro-electronic applications like blocking materials for microwave package, high voltage contact materials, and heat sink materials for high-density integrated circuits. Their observations showed that increasing the Cu content to 30 wt % caused the electrical resistivity to decrease, which corresponded directly to the addition of Cu having high electrical conductivity. Increasing temperature produced an increase in electrical resistivity. They found that the thermal conductivity of metal could be approximated by the sum of two terms, i.e. a residual component and a thermal component. As a result, a larger number of thermally excited elastic waves, called photons, scatter conduction electrons and decrease the relaxation time between collisions.

Koráb *et al.* [64] investigated the thermal conductivity of unidirectional copper matrix-carbon fibre composites. The thermal conductivity of these composites is characterized and analyzed in directions parallel and transverse to the carbon fibre orientation. Unidirectional samples with different fibre content were produced by diffusion bonding of continuous copper-coated carbon fibre tows. The conductivity decreased with increasing fibre content. The low transverse thermal conductivity of the Cu-C_f composite was due to a broken copper network and the low thermal conductivity of the fibre.

Brito and Sánchez [65] studied the influence of metallic fillers (copper, zinc, and aluminum) on the thermal and mechanical behaviour of composites with an epoxy matrix. In the filled materials, various percentages (10 %, 20 % and 30 % by weight) were used. Samples with and without metallic fillers, and three epoxy-amine molar ratios (1:1, 1:1.5 and 2:1) were selected. The results show that at 10 % of the filler, the composite with copper showed the highest breaking strength for all the studied ratios. At the epoxy/amine ratios 2:1 and 1:1.5 with 20 and 30 % of the filler the composite with Al presented the highest breaking strength. Such effects can be attributed to strong filler-matrix adhesion. The filler decreased the thermal stability of the diglycidylether of bisphenol "A" (DGEBA)/ethylenediamine (ETDA) matrix.

Gaier *et al.* [66] investigated the electrical and thermal conductivity of woven pristine and intercalated graphite fibre-polymer composites. To date the high electrical and thermal conductivity of laminar carbon fibre-polymer composites have been largely overlooked when designing aerospace structures. This was in spite of the fact that high-grade graphite fibres have thermal conductivities exceeding that of metals [67], and when modified by intercalation, have electrical conductivity comparable to metals [68], but at much lower mass

density and higher strengths and moduli. The resistivity measured on a narrow composite strip revealed a dependence on the angle of measurement with respect to the weave direction. The angular dependence on the resistivity fits a very simple model. The first assumption of the model was that the current travel only along the axis of the fibres, i.e. the transverse resistivity of the fibres was much higher than the axial resistivity. This was supported by measurements in metal matrix composites, which indicate that the transverse resistivity of the fibre is about 10^2 times higher than the axial resistivity [69]. The current can only transverse one fibre diameter, and then it must travel through the resin, which has a very high resistivity ($> 10^{13} \Omega \text{ cm}$). The second assumption was that the contact resistance between fibres within the weave was negligible, because each axial fibre crosses several thousand transverse fibres, in effect a parallel circuit of several thousand resistors. Qualitatively, the thermal conductivity results mirrored the electrical resistivity, and the thermal conductivity of composites made from the most highly conductive fibre was much lower than that predicted by the rule of mixtures. This was thought to be an artifact of the measurement technique employed.

Yu *et al.* [70] studied the thermal conductivity of polymer composites having a matrix of polystyrene (PS) containing aluminum nitride (AlN) reinforcement. The results showed that the polystyrene particles were essentially surrounded by AlN powder, although there was some connectivity between adjacent polystyrene particles in small regions. The particle size of the polystyrene matrix had an effect on the thermal conductivity of the composites in this dispersion state. Larger polystyrene particles gave rise to a higher thermal conductivity of the composites. Addition of aluminum nitride resulted in a continuous increase in the thermal conductivity of the composites. In the present study, polystyrene composite with aluminum nitride have been prepared. A special dispersion state of the filler was achieved in these composites in which the polystyrene particle are surrounded by aluminum nitride particle. The results show that it is possible to improve the thermal conductivity of the polymer at low filler contents with this kind of dispersion, so that the adverse effect of the filler on the dielectric properties of the polymer composites may be minimized.

Agari *et al.* [71] investigated polyethylene composites filled with graphite, prepared by using four dispersion methods:

- (a) Powder mix: mixing the powders of polyethylene and graphite.
- (b) Solution mix: dispersing graphite into polyethylene dissolved in toluene.
- (c) Roll-milled mix: melting of polyethylene kneaded with graphite on a roll mill.
- (d) Melt mix: dispersing graphite in molten polyethylene.

They found that, for a given volume fraction of graphite, the thermal conductivity of polyethylene composites were ranked as follows: powder mixture > solution mixture > roll-milled mixture > melted mixture.

Krupa and Chodak [72] investigated the physical properties of thermoplastic/graphite composites. The thermal and electrical conductivity, as well as thermal diffusivity of HDPE/graphite and polystyrene/graphite composites were investigated. Two grades of graphite (EG-10, synthetic graphite, SGL carbon, UK and KS-15, synthetic graphite, Lonza, Switzerland) were used as fillers. A nonlinear increase in thermal conductivity was observed with an increase in graphite content, and the thermal conductivity of composites containing graphite KS-15 was higher than that of composites containing the same concentration of graphite EG-10. This difference is more significant for the PS matrix, especially at higher filler concentration. Since thermal conductivity should not depend on the size of the particles [73, 74], the most probable explanation is that more conductive paths are created because of higher agglomeration of graphite KS-15. The results show that the thermal conductivity of HDPE is higher than the thermal conductivity of PS. Semi-crystalline matrices have higher thermal conductivity compared to amorphous matrices, since the crystalline phase enables a better transport than the amorphous phase.

Several models have already been developed to describe the thermal conductivity of composites [73, 74], but none of them has general validity. The models can be divided into three groups. The first is based on an exact approach to the problem of transport of heat using an effective medium approximation. The second one deals with a calculation of the upper and lower boundaries, and the last one is based on the bond percolation theory [95]. The models based on the effective medium approximation as well as the boundary calculations often fail if the thermal conductivity of the filler is substantially different from that of the matrix (by more than one order of magnitude). This is also the case for other properties [96]. Other known models, that correlate thermal conductivity with the ability of the filler to create infinite clusters of particles is that of Agari *et al.* [97, 98] and Wunderlich [99]. The thermal conductivity is generally described by Equation 3.1.

$$\log \lambda_c = \phi_f c_2 \log \lambda_f + (1 - \phi_f) \log (c_1 \lambda_m) \quad (3.1)$$

where λ_c , λ_m , λ_f are the thermal conductivities of the composite, matrix, and filler, ϕ_f is the volume portion for the filler and the parameter c_2 characterizes the ability of the filler particles

to create an infinite cluster. Parameter c_1 is related to the change in thermal conductivity of a semicrystalline matrix, as a consequence of a change in the degree of crystallinity.

Weidenfeller *et al.* [75] investigated the thermal conductivity, thermal diffusivity, and specific heat capacity of particle-filled polypropylene. As filler materials copper, talc, magnetite, strontium ferrite, barite and glass fibers were selected to vary over a broad range of different filler properties, ranging from 2.58 (glass fibers) to 8.94 g cm⁻³ (copper) in density, and from nearly 1.5 (glass fibers) to approximately 400 W m⁻¹ K⁻¹ (copper) in thermal conductivity. The highest thermal conductivity of a composite was achieved with talc which has a moderate thermal conductivity ($\lambda_{\text{talc}} \approx 10.6 \text{ W m}^{-1} \text{ K}^{-1}$) compared to the high thermal conductivity of copper ($\lambda_{\text{copper}} \approx 400 \text{ W m}^{-1} \text{ K}^{-1}$). The thermal conductivity of the talc-filled polymer increased from 0.27 to 2.50 W m⁻¹ K⁻¹ with 30 vol % talc filler. This behaviour is a consequence of the microstructure of talc-filled PP showing a high interconnectivity of the talc crystals. On the other hand, the thermal conductivity of copper-filled polypropylene is, in spite of the very high conductivity of pure copper, lower than that of talc-filled PP composites due to the poor interconnectivity of the Cu-particles. The talc platelets and the glass fibres were aligned in the test samples by the injection molding process. This led to a thermal conductivity close to the upper boundary according the Hashin and Shtrikman (HS) model [76], and simulated a talc matrix and a glass matrix, respectively, which surrounded the polypropylene particles. In addition, the specific heat capacities and thermal diffusivities of talc-filled polypropylene were much higher than those of copper filled polypropylene. A comparison of the two competing materials, barite and magnetite, for increasing the weight of polymers, showed for magnetite-filled PP a higher thermal conductivity than for barite-filled PP. This resulted not only from small differences in specific density, but also from lower specific heat capacity and thermal diffusivity of barite-filled PP compared with magnetite-filled PP. The significant lower thermal conductivity of the barite-filled PP compared to the magnetite-filled one could be directly related to the substantially lower thermal conductivity of barite ($\approx 2 \text{ W m}^{-1} \text{ K}^{-1}$) compared to the higher conductivity of magnetite ($\approx 5 \text{ W m}^{-1} \text{ K}^{-1}$). Furthermore, the higher interconnectivity of magnetite-filled PP increased the thermal conductivity of the composite compared to the barite-filled one. In the temperature range from 300 to 385 K the specific heat capacity of the composites was increased for PP with magnetite (from 1.20 up to 1.87 J g⁻¹ K⁻¹) and for PP with barite fillers (from 0.77 up to 1.29 J g⁻¹ K⁻¹). In the same temperature region, the thermal diffusivity decreases. This study indicates that, for injection molding processes of heavy plastic composites, magnetite might be a good choice, as it allows higher production cycles than the barite-filled composites. To increase the

thermal conductivity significantly without increasing the density very much, talc-filled composites seem to be a good candidate and can help to save cooling time during the injection molding process.

1.6 Mechanical properties

Baré *et al.* [77] investigated the effect of irradiation on the mechanical properties of HDPE reinforced with carbon steel and copper fibres. The sample was irradiated with a ^{60}Co source at doses between 10 and 70 kJ kg^{-1} (kGy) using an irradiation rate of 4.8 $\text{kJ kg}^{-1} \text{h}^{-1}$ in an oxygen atmosphere at room temperature. The results show that, at lower irradiation doses, the mechanical properties of the material were positively affected; reaching their highest values at approximated 10 kJ kg^{-1} . For the pure HDPE, Young's modulus increased up to 100 % independent of the irradiation dose, while for the polymer containing metallic fibres this parameter increased to approximately 200 %, and the impact resistance increased by up to 600 % due to the presence of the metallic fibres.

Chodák and Krupa [78] investigated the percolation effect and mechanical behaviour of carbon black filled polyethylene. The results show that the presence of the filler resulted in both an easier initiation of crack formation *via* stress concentration on the filler surface, and a decrease in chain mobility due to polymer-filler interaction, resulting in lower deformation of the material. Both effects contribute to a decrease in the elongation at break values.

Fan *et al.* [79] investigated the thermal, electrical and mechanical properties of plasticized polymer electrolytes based on poly(ethylene oxide) (PEO)/poly(vinylidene fluoride-co-hexafluoropropylene (P(VDF-HFP))). They observed that, when the plasticizer content increased, the electrolytes showed a dramatic decrease in their elongation at break values and critical stresses, and when a small amount of PEO was added to the film, it showed a large increase in both critical stress and elongation at break values. The mechanical strength of the plasticized polymer electrolytes depended on both the ratio of PEO/P(VDF-HFP) and the plasticizer content.

Bloom *et al.* [80] investigated the fabrication and wear resistance of Al-Cu-Fe quasicrystal-epoxy composite materials. Novalac epoxy filled with Al-Cu-Fe quasicrystal powders were evaluated by pin-on-disk testing using 52100 steel counterfaces. The addition of a particulate filler, often a ceramic, metal or polymer, led to the production of materials with increased strength and wearability when compared to their unfilled counterparts. High-speed steels that incorporate Al_2O_3 and TiN-coated Al_2O_3 particles, were found to have

excellent wear resistance under dry sliding conditions [81]. Durand *et al.* [82] demonstrated similar improvements in the wear resistance for epoxies filled with Al_2O_3 , and noted that while their interests were to evaluate the role of ceramic particles for metal matrix composites, there were no wear studies of ceramic filled epoxies in the literature. While ceramic particles increased the wear resistance of the epoxy, they were rough to the 52100 steel counterface (700 HV_{10}). In order to achieve low wear on both mating surfaces, the aluminum oxide counterface (1900 HV_{10}) is required.

Anderson *et al.* [83] investigated Al–Cu–Fe quasicrystal/ultra-high molecular weight polyethylene composites as biomaterials for acetabular cup prosthetics. The wear properties of the Al–Cu–Fe/UHMWPE samples and a 440 steel ball counterface were measured. The mechanical strength of the Al–Cu–Fe/UHMWPE composites was compared to UHMWPE and alumina/UHMWPE. The wear on both the substrate and the counterface for the alumina/UHMWPE samples was much higher than that of either the UHMWPE or Al–Cu–Fe/UHMWPE samples. Dynamic mechanical analysis determined that the mechanical strength, represented by the storage modulus and $\tan \delta$, was improved by the addition of the Al–Cu–Fe quasicrystals to UHMWPE. The storage modulus increased by over 25 % at 37 °C, and $\tan \delta$ was lower over the entire temperature range for the Al–Cu–Fe/UHMWPE relative to the UHMWPE. Direct contact cytotoxicity tests revealed that the Al–Cu–Fe/UHMWPE composites elicited the same cytotoxic response as pure UHMWPE that is routinely used for acetabular cup prosthetics.

Kim *et al.* [84] investigated the characteristics of a carbon fibre phenolic composite for journal bearing materials. In this study, a hybrid composite journal bearing composed of a carbon fibre reinforced phenolic composite liner and a metal backing was manufactured to solve the seizure problem of metallic journal bearing materials, because the carbon fibre has a self-lubricating ability and the phenolic resin has thermal resistance characteristics. To estimate the wear resistance of carbon fibre phenolic composite, wear tests were performed at several pressures and velocities. The oil absorption characteristics, coefficient of thermal expansion, strength and stiffness of the composite were also tested. Using the measured stiffness values, the thermal residual stresses in the composite were calculated to check the reliability of the composite journal bearing. The friction and wear characteristics of the carbon fibre reinforced phenolic composites and the asbestos fibre reinforced phenolic composites were measured, and it was found that the former had superior characteristics to that of the latter. Especially, the carbon fibre reinforced phenolic composites was not susceptible to change of load and velocity under the same PV value (P : pressure, V : speed). The wear

volume of the carbon fibre reinforced composites, saturated with oil, was less than half of the dry specimen. The dry friction coefficient of carbon fibre reinforced phenolic was about 60 % of the asbestos fibre reinforced phenolic under the same PV value. The safety of the hybrid composite journal bearing was verified by stress analysis results. It was found that the hybrid composite journal bearing may solve the problems of conventional journal bearings such as white metal lining and polymeric journal bearings.

Bloom *et al.* [85] investigated the development of novel polymer/quasicrystal composite materials. The results indicate that new composites are a means of enhancing the properties of certain organic polymers, while providing a new means of processing quasicrystals. Al–Cu–Fe gas atomized powder was used as reinforcing filler in the polymer matrices of this study. The addition of Al–Cu–Fe quasicrystal (QC) rich powder to amorphous, semicrystalline, and thermosetting polymers showed improved wear resistance to volume loss compared to the unfilled polymers. The corresponding reduction in wear was attributed to the low coefficient of friction and high hardness of the quasicrystal rich powders. The storage modulus (E') of the composite materials was found to increase with increasing volume fraction of the quasicrystal powder, as expected for a filled polymer composite containing rigid fillers [86].

Weick and Bhushan [87] investigated the relationship between dynamic mechanical behaviour, transverse curvature, and wear of magnetic tapes. Five types of tapes were analyzed including three polyethylene terephthalate (PET) tapes with metal particulate, barium ferrite particulate, and metal-evaporated coatings. A polyethylene naphthalate (PEN) tape with a barium ferrite particulate coating was also analyzed along with an aromatic polyamide (ARAMID) tape with a metal-evaporated coating. From the dynamic mechanical analysis (DMA), the storage (or elastic) modulus, E' , was obtained as a function of temperature and frequency along with the loss tangent, $\tan \delta$, which is a measurement of viscous energy dissipation. Frequency-temperature superposition was used to predict the dynamic mechanical behavior of the tapes and substrates over a 10-12 decade frequency range. The results show that the advanced PEN and ARAMID tapes tended to have higher storage moduli than the PET tapes, and the PET tapes were more susceptible to non-recoverable deformation at higher frequencies due to their higher loss tangents. The storage moduli for the tapes were typically higher than those for the substrates, due to the role that the particulate or metal-evaporated coatings played in increasing the overall modulus of the tapes. Tapes with particulate coatings had higher loss tangents than their constitutive substrates, whereas ultra-thin metal-evaporated coatings contributed little to the loss tangent behaviour of

a tape. The DMA data was used in a model to predict the resistance of a tape to transverse curvature when tension was applied. The transverse curvature of a magnetic tape is related to higher edge wear of a head.

1.7 Surface energy

Surface energy evaluation is used in various fields. The surface properties of polymers play a major role in applications such as blending, adhesion, and coatings. There is however, not much known about the surface energy of metal-filled polymers. The adhesive bond between paint or adhesive and a substrate requires the establishment of interfacial molecular contact by wetting. One of the important characteristics of a liquid penetrant material is its ability to freely wet the surface of the object being inspected. At the liquid-solid surface interface, if the molecules of the liquid have a stronger attraction to the molecules of the solid surface than to each other, the adhesive forces are stronger than the cohesive forces, and wetting of the surface occurs. Alternatively, if the liquid molecules are more strongly attracted to each other than to the molecules of the solid surface, the cohesive forces are stronger than the adhesive forces, and the liquid beads up and do not wet the surface. One way to quantify a liquid's surface wetting characteristics is to measure the contact angle of a drop of liquid placed on the surface of the solid object. The contact angle is the angle formed by the solid-liquid interface and the liquid-vapor interface measured from the side of the liquid. Liquids wet surfaces when the contact angle is less than 90 degrees. For a penetrant material to be effective, the contact angle should be as small as possible, that for liquid penetrants are very close to zero degrees [88].

Jintang [89] investigated the friction and wear on various polymers/stainless steel, PTFE/various metals and JS material (a multilayer composite)/stainless steel composites. The XPS spectra and atomic relative concentrations of elements on mating surfaces, the EPM spectra of element line distributions on frictional surfaces and the ESR spectra of radicals in polymer wear debris were determined. The test results indicated that polymer transfer films were formed on all friction surfaces. Meanwhile, extremely complex tribochemical reactions took place on the interfaces. The friction and wear properties of polymer were closely related to the adherent strength and covering extent of the transfer film on the counterface. The transfer film formation was influenced by polymer structure characteristics, tribochemical reactions and friction conditions.

Marzouk *et al.* [90] studied the non-selective copper film growth on polyimide by reduced-pressure (20 Torr) metal organic chemical vapor deposition (MOCVD). In the first few minutes of deposition, the deposition film consisted entirely of the copper oxide phase. As the reactions continued, pure copper films were obtained. The simple scotch-tape adhesion tests revealed qualitatively that the deposited films adhere well to the polyimide substrate.

1.8 Polarized optical microscopy

Oriented polymeric structures often exhibit optical birefringence [91] as a result of the difference in polarization along and across the molecular backbone. Orientation in polymers and liquid crystals is often investigated in conventional far-field microscopy using polarized light. The simplest method for the study of birefringence is crossed-polar arrangement, in which the specimen is placed between a polarizer and an analyzer, the electric vectors of which are rotated through $\pi/2$ with respect to each other. With no specimen between the crossed polars, no light is transmitted through the optical system. When a birefringent specimen is placed between the crossed polar with its anisotropic axis at some angle θ to the electric vector of polarized light, the transmitted intensity varies with θ according to $\sin^2(2\theta)$. Thus, in a specimen of uniform thickness, regions of different molecular orientation appear with different intensities in the microscope.

Polarized light microscopy is known for its geological applications, primarily for the study of minerals in rock thin sections, but it can also be used to study both natural and industrial minerals whether refined, extracted or manufactured, composites such as cements, ceramics, mineral fibres and polymers, and crystalline or highly ordered biological molecules such as DNA, starch, wood and urea. Most of the techniques developed in conventional far-field optical microscopy can be transferred to scanning near-field optical microscopy (SNOM). The instrument incorporates a non-contact force control system [92] so that topographic and optical data can be collected simultaneously.

Williamson and Miles [93] studied the molecular orientation in polymers from near-field optical polarization measurements. Using polarized light, the birefringence structure of the spherulite revealed a concentric ring structure with sub-micron resolution. They found that the optical images could be correlated with the topographic images, recorded simultaneously, of the same area. This demonstrated directly the correlation between the twisting structure of ribbon-like polymer crystallites and the birefringent concentric ring structure, and

demonstrates the capability of scanning near-field optical microscopy for studying molecular orientation as a function of topographic structure.

1.9 Aim and scope of this work

Fillers play an important role in the production of polymeric materials. In addition to cost saving, other value-added properties are gained through the use of fillers. Fillers can improve the physical, rheological, chemical resistance, thermal, optical and electrical properties of a polymeric material. The electrical and thermal conductivity of polymers can be increased with the addition of a metallic filler. Polymer composites can be modified for more specific uses including anti-fouling compounds, corrosion-resistant paints, maintenance and repair products, such as cold-poured steel and tooling with the use of metallic fillers in the polymer matrix.

Metal filled polymer composites are widely used for electromagnetic interference shielding. They have a lighter weight than metals and are less costly. The physical properties and the percentage of the filler materials must be known in order to determine the usefulness of the materials. It is therefore important, from a scientific and practical point of view, to understand the effects of a metallic filler on the properties of a polymer matrix.

The aim of this study was to investigate the thermal, mechanical and electrical properties of copper powder filled polyethylene composites. Thermal and mechanical properties, electric and thermal conductivity, as well as the surface properties and optical appearance of the samples were determined. The influence on these properties of the amount of copper powder in the polymer matrix will be discussed.

CHAPTER TWO

MATERIALS AND METHODS

2.1 Materials

2.1.1 Polyethylene

Low-density and linear low-density polyethylenes were used as the matrix components. Sasol Polymers, South Africa, supplied these polymers. The LDPE has an MFI of 7.0 g / 10 min, a melting temperature of 106 °C, a molecular weight of 96 000 g mol⁻¹, and a density of 0.918 g cm⁻³. The LLDPE has an MFI of 1.0 g / 10 min, a molecular weight of 191 600 g mol⁻¹, a melting temperature of 124 °C, and a density of 0.924 g cm⁻³.

2.1.2 Copper powder

Merck Chemicals in South Africa supplied copper powder, which was used as the filler component. It has a melting point of 1083 °C and a density of 8.96 g cm⁻³. The particle sizes were < 38 μm.

2.2 Methods

2.2.1 Preparation of composites

The composites were prepared by mixing the polymer and copper powder in a Brabender Plastograph at different ratios (Table 2.1). Samples were weighed according to the required ratios, and mixed in a 55 cm³ mixing chamber at 160 °C and a speed of 30 rpm for 10 minutes. The volumes of PE and copper to be mixed were obtained from the ratios in Table 2.1 and Equation 2.1.

$$V = V_1 + V_2 = 55 \text{ cm}^3 \quad (2.1)$$

where V is the volume of the mixing chamber of the Brabender Plastograph, V_1 the volume of the filler (Cu) and V_2 the volume of PE. The respective volumes were calculated and substituted in Equation 2.2 to get the required masses to be mixed.

$$m = (V/\text{cm}^3) \times (\rho/\text{g cm}^{-3}) \times K \quad (2.2)$$

where m is the mass of the component, V the volume of the component, ρ its density, and K a constant which is referred to as a non-dimensional coefficient which considers the optimum filling level for different dynamic loads. This factor is usually smaller than 1 and, based on this, the recommended value for initial tests is 0.7. To calculate the mass values required for LLDPE-Cu and LDPE-Cu, Equation 2.2 was used. After preparation, the samples were melt pressed at 160 °C for 10 minutes, and were allowed to cool for 10 minutes at room temperature.

Table 2.1 Compositions of composite samples

PE-Cu (V/V)	PE-Cu (V/V)
100-0	90-10
99-1	88-12
98-2	84-16
97-3	82-18
96-4	78-22
95-5	76-24

2.2.2 Differential scanning calorimetry (DSC)

DSC analyses were performed in a Perkin-Elmer DSC 7 under flowing nitrogen. The instrument was computer controlled and calculations were done using Pyris software. The instrument was calibrated using the onset temperatures of melting of indium and zinc standards, as well as the melting enthalpy of indium. 5-10 mg samples were sealed in aluminium pans and heated from 25 to 160 °C at a heating rate of 10 °C min⁻¹, and cooled at the same rate to 25 °C. For the second scan, the samples were heated and cooled under the

same conditions. Onset and peak temperatures of melting and crystallization, as well as melting and crystallization enthalpies were determined from the second scan.

2.2.3 Thermogravimetric analysis (TGA)

Thermogravimetric analyses were carried out in a Perkin-Elmer TGA7 thermogravimetric analyzer under flowing nitrogen. The instrument was computer controlled and calculations were done using Pyris software. Samples of 5-10 mg were heated from 25 to 600 °C at 20 °C min⁻¹. The instrument uses mass % on the y-axis of the TGA curve.

2.2.4 Tensile testing

A Hounsfield H5KS tensile tester was used for the tensile analysis of the samples. The dumbbell samples were stretched at a speed of 50 mm min⁻¹ under a cell load of 2500 N. The gauge length was 24 mm, the thickness ranged between 0.5 and 1.0 mm, and the width was 4.8 mm. The final mechanical properties were evaluated from 5 different measurements.

2.2.5 Surface free energy testing

For the determination of the total surface free energy of the samples, as well as its disperse and polar parts, a surface energy evaluation system (SEES, Czech Republic) was used, which is able to determine the polar and dispersed components of the total surface energy with standard deviations. In this work, contact angle measurements were done by a drop method using the Owens-Wendt regression method. Five liquids of different polarity (benzyl alcohol, aniline, formamid, ethylene glycol) were used. For each measurement, 15 drops of each of the liquids were used to ensure reproducibility at room temperature.

2.2.6 Electrical conductivity

The volume electrical conductivity in the polymer composites was measured according to ASTM D257. A three-electrode electrometer arrangement was used for the DC measurements of the resistance. A voltage of 500 V was used, due to a very low level of electrical conductivity. An electro-conductive solution was used to achieve good electrical contact between the sample surface and the electrode of the conduction tester.

2.2.7 Thermal conductivity

The thermal conductivity was measured using a multipurpose apparatus (ISOMET, Applied Precision, Bratislava, Slovakia) for non-steady measurements of thermal properties. The data are calculated automatically from a time dependence of the thermal flow in the material. Measurements were made at 25 ± 2 °C with a flat probe.

Thermal conductivity is a property of materials that expresses the heat flux f (W m^{-2}) that will flow through the material if a certain temperature gradient DT (K m^{-1}) which exists over the material. The thermal conductivity (λ) is usually expressed in $\text{W m}^{-1} \text{K}^{-1}$. Equation 2.3 was used for the calculation of the thermal conductivity.

$$f = \lambda \times DT \quad (2.3)$$

2.2.8 Polarized optical microscopy

Polarized optical micrograms were taken at 100x and 400x magnifications, using a CETI polarized optical microscope, made in Belgium. The photographs were taken with a Ceist DCM digital camera. The samples were placed on a glass plate for analysis.

CHAPTER THREE

RESULTS AND DISCUSSION

3.1 Polarized optical microscopy

Optical micrograms of different Cu/PE composites, at different magnifications, are shown in Figure 3.1. The copper powder particle distributions are relatively uniform at both low and high copper contents, although not completely homogeneous. There are, however, large variations in copper particle size distributions. Figure 3.1 (b, c, f and g) shows cluster formation of copper particles at higher Cu contents. Figure 3.1 (c and f) also shows the formation of percolation paths of copper in the PE matrices.

3.2 Surface free energy

The surface free energy values of the pure polyethylenes and their different composites are presented in Table 3.1. These values are plotted in Figures 3.2 (LDPE) and 3.3 (LLDPE). These results show an increase in the total surface free energy and its disperse part, but a decrease in the polar part of the surface free energy for the Cu-PE composites in comparison with pure PE. The respective increase and decrease of values is relatively strong after addition of low amounts of copper, whereafter the values slightly increase up to 18 vol.% copper in the composites. Polyethylene is known to be non-polar, and the presence of copper filler further reduces the polarity.

Table 3.1 The surface free energy, as well as its disperse and polar parts, of the different samples (g_{SE} = total, g_{LW} = disperse, g_{AB} = polar)

LDPE-Cu				LLDPE-Cu			
Vol.% Cu	g_{SE}	g_{LW}	g_{AB}	Vol.% Cu	g_{SE}	g_{LW}	g_{AB}
0	31.8 ± 1.8	28.5 ± 1.2	3.3 ± 0.2	0	39.8 ± 2.2	36.7 ± 2.1	3.1 ± 0.2
3	32.3 ± 1.9	29.9 ± 1.0	1.4 ± 0.3	3	40.7 ± 3.1	39.1 ± 2.7	1.5 ± 1.3
5	34.1 ± 2.0	32.5 ± 2.5	1.5 ± 0.4	5	40.6 ± 2.7	38.4 ± 2.7	2.2 ± 2.2
18	34.3 ± 2.0	32.7 ± 1.0	1.8 ± 0.4	18	40.6 ± 2.5	38.5 ± 2.5	2.4 ± 2.2

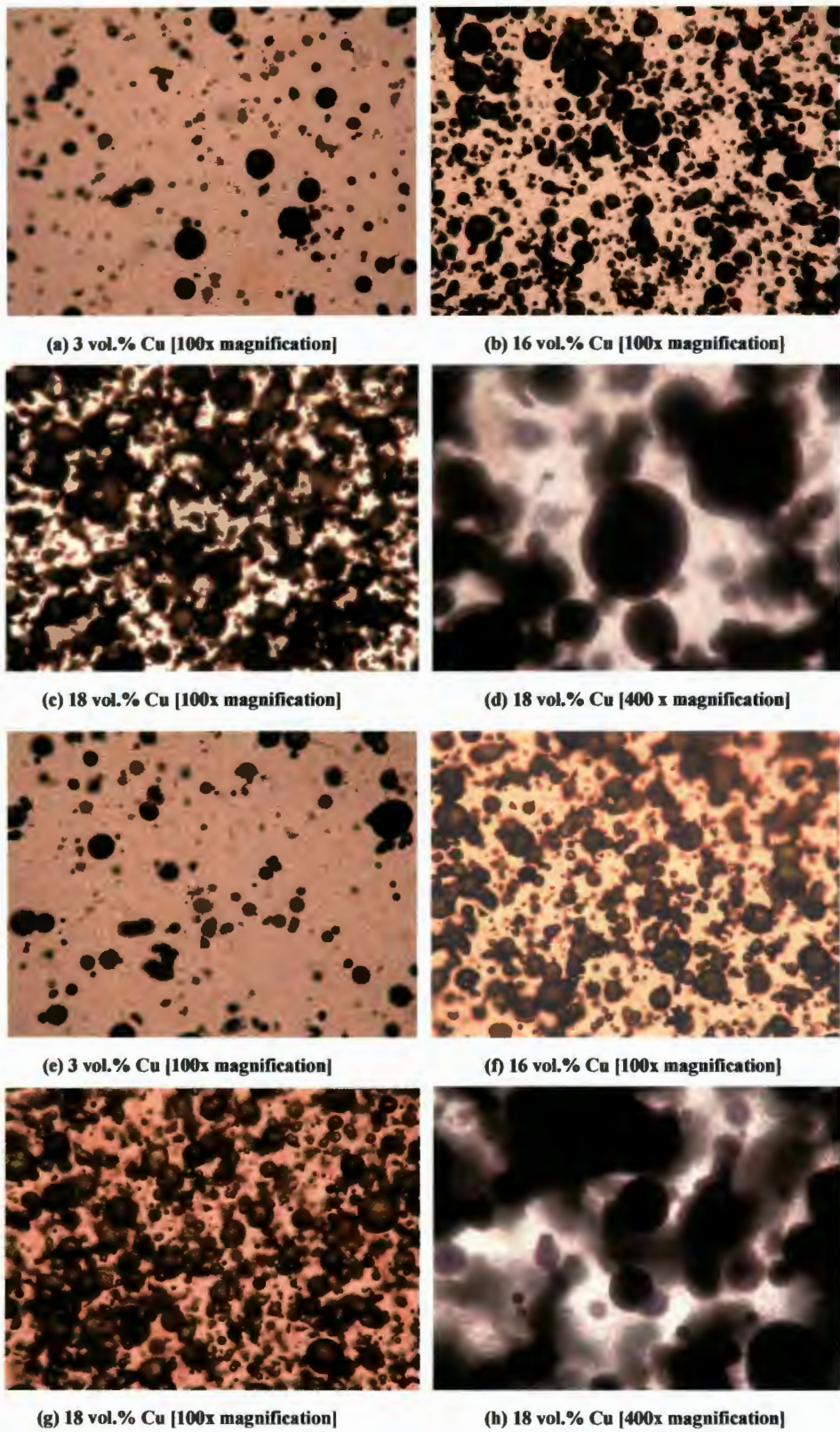


Figure 3.1 Polarized optical micrograms of polyethylene-copper composites (LDPE composites: a – d, LLDPE composites: e – h)

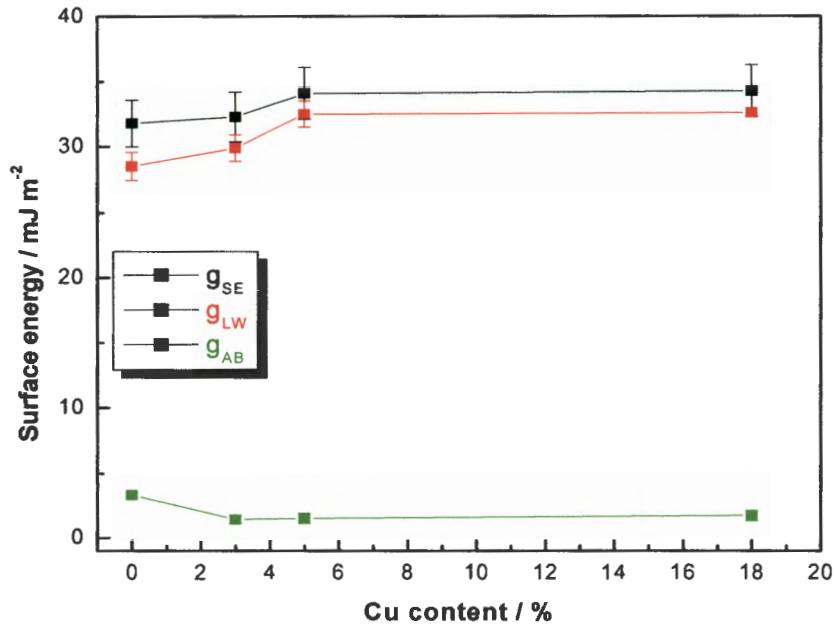


Figure 3.2 The variation of surface energy, as well as its disperse and polar parts, of LDPE-copper composites (g_{SE} = total, g_{LW} = disperse, g_{AB} = polar)

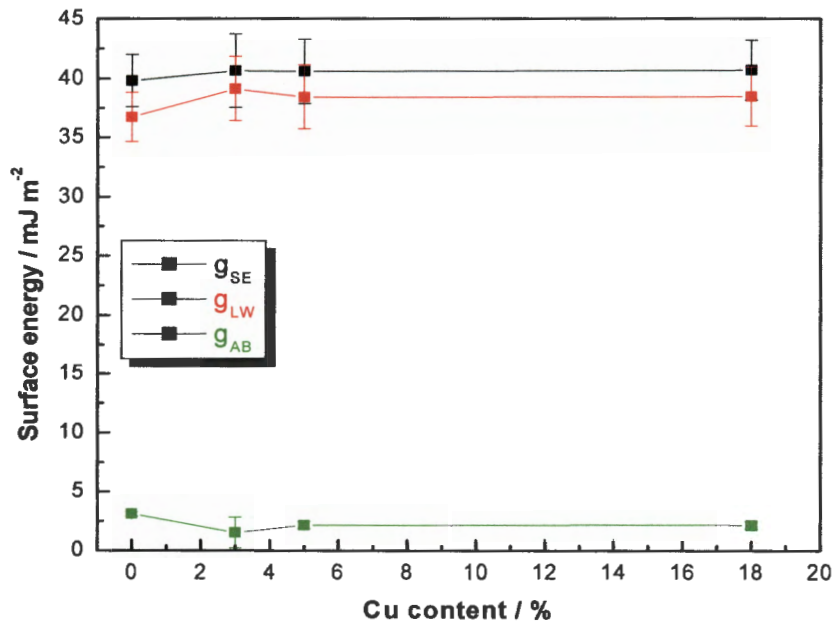


Figure 3.3 The variation of surface energy, as well as its disperse and polar parts, of LLDPE-copper composites (g_{SE} = total, g_{LW} = disperse, g_{AB} = polar)

3.3 Thermal properties

3.3.1 Differential scanning calorimetry (DSC)

The DSC curves are shown in Figures 3.3 – 3.5, and the results are summarized in Tables 3.2 and 3.3. The figures show only one melting and one crystallization peak for each sample. Pure LDPE has a melting peak temperature of 103.2 °C, and this temperature initially increases to 107.4 °C for the composite containing 1 vol.% Cu, after which it gradually decreases to 103.7 °C as the Cu content in the samples increases. This is the result of changing lamellar thickness, which is due to additional crystallization in the presence of copper. It may be explained through LDPE chains in the amorphous phase crystallizing epitaxially on the copper particle surfaces. The enthalpy data (Table 3.2), where the observed enthalpy is compared with the expected enthalpy (calculated taking into account the weight fraction of LDPE in the samples, and assuming that the LDPE crystallization mechanism does not change in the presence of copper), indicates a higher enthalpy in the presence of low copper contents. This indicated higher crystallinity, which supports the explanation above.

Table 3.2 DSC data of LDPE-Cu composites

Vol.% Cu	First heating				Second heating				Cooling		
	$T_{o,m} /$ °C	$T_{p,m} /$ °C	$\Delta H_m^{obs} /$ J g ⁻¹	$\Delta H_m^{exp} /$ J g ⁻¹	$T_{o,m} /$ °C	$T_{p,m} /$ °C	$\Delta H_m^{obs} /$ J g ⁻¹	$\Delta H_m^{exp} /$ J g ⁻¹	$T_{o,c} /$ °C	$T_{p,c} /$ °C	$\Delta H_c /$ J g ⁻¹
0	96.8	103.3	58.3	-	96.1	103.2	52.5	-	89.9	86.3	-41.8
1	100.5	107.2	57.0	53.1	101.0	107.4	52.0	47.8	94.9	92.0	-41.4
2	100.5	106.5	52.8	48.6	100.8	106.9	46.0	43.7	95.1	92.3	-33.7
3	100.6	106.2	42.8	44.8	100.6	106.7	45.2	40.4	95.3	92.6	-30.4
4	99.9	105.7	40.7	41.4	100.7	106.5	38.8	37.3	95.1	92.3	-31.5
5	100.1	106.7	41.4	34.5	100.8	107.0	37.8	34.7	94.9	92.1	-24.6
12	97.0	105.7	31.6	25.1	95.3	104.1	24.2	22.6	91.3	85.6	-15.5
16	95.9	103.7	19.3	20.4	95.6	103.7	21.9	18.4	92.1	86.6	-16.1
18	97.2	103.3	15.5	18.7	95.3	103.4	20.7	16.8	91.1	85.9	-11.8
24	93.4	103.4	16.2	14.5	96.9	103.7	15.7	13.1	86.6	83.3	-13.9

$T_{o,m}$ – onset temp. of melting, $T_{p,m}$ – peak temp. of melting, ΔH_m – melting enthalpy, $T_{o,c}$ – onset temp. of crystallization, $T_{p,c}$ – peak temp. of crystallization, ΔH_c – crystallization enthalpy, obs – observed, exp - expected

3.3 Thermal properties

3.3.1 Differential scanning calorimetry (DSC)

The DSC curves are shown in Figures 3.3 – 3.5, and the results are summarized in Tables 3.2 and 3.3. The figures show only one melting and one crystallization peak for each sample. Pure LDPE has a melting peak temperature of 103.2 °C, and this temperature initially increases to 107.4 °C for the composite containing 1 vol.% Cu, after which it gradually decreases to 103.7 °C as the Cu content in the samples increases. This is the result of changing lamellar thickness, which is due to additional crystallization in the presence of copper. It may be explained through LDPE chains in the amorphous phase crystallizing epitaxially on the copper particle surfaces. The enthalpy data (Table 3.2), where the observed enthalpy is compared with the expected enthalpy (calculated taking into account the weight fraction of LDPE in the samples, and assuming that the LDPE crystallization mechanism does not change in the presence of copper), indicates a higher enthalpy in the presence of low copper contents. This indicated higher crystallinity, which supports the explanation above.

Table 3.2 DSC data of LDPE-Cu composites

Vol.% Cu	First heating				Second heating				Cooling		
	$T_{o,m}$ / °C	$T_{p,m}$ / °C	ΔH_m^{obs} / J g ⁻¹	ΔH_m^{exp} / J g ⁻¹	$T_{o,m}$ / °C	$T_{p,m}$ / °C	ΔH_m^{obs} / J g ⁻¹	ΔH_m^{exp} / J g ⁻¹	$T_{o,c}$ / °C	$T_{p,c}$ / °C	ΔH_c / J g ⁻¹
0	96.8	103.3	58.3	-	96.1	103.2	52.5	-	89.9	86.3	-41.8
1	100.5	107.2	57.0	53.1	101.0	107.4	52.0	47.8	94.9	92.0	-41.4
2	100.5	106.5	52.8	48.6	100.8	106.9	46.0	43.7	95.1	92.3	-33.7
3	100.6	106.2	42.8	44.8	100.6	106.7	45.2	40.4	95.3	92.6	-30.4
4	99.9	105.7	40.7	41.4	100.7	106.5	38.8	37.3	95.1	92.3	-31.5
5	100.1	106.7	41.4	34.5	100.8	107.0	37.8	34.7	94.9	92.1	-24.6
12	97.0	105.7	31.6	25.1	95.3	104.1	24.2	22.6	91.3	85.6	-15.5
16	95.9	103.7	19.3	20.4	95.6	103.7	21.9	18.4	92.1	86.6	-16.1
18	97.2	103.3	15.5	18.7	95.3	103.4	20.7	16.8	91.1	85.9	-11.8
24	93.4	103.4	16.2	14.5	96.9	103.7	15.7	13.1	86.6	83.3	-13.9

$T_{o,m}$ – onset temp. of melting, $T_{p,m}$ – peak temp. of melting, ΔH_m – melting enthalpy, $T_{o,c}$ – onset temp. of crystallization, $T_{p,c}$ – peak temp. of crystallization, ΔH_c – crystallization enthalpy, obs – observed, exp – expected

and 3.3. Since copper has a relatively high heat capacity, its presence in high contents has an influence on the heat transport in the samples.

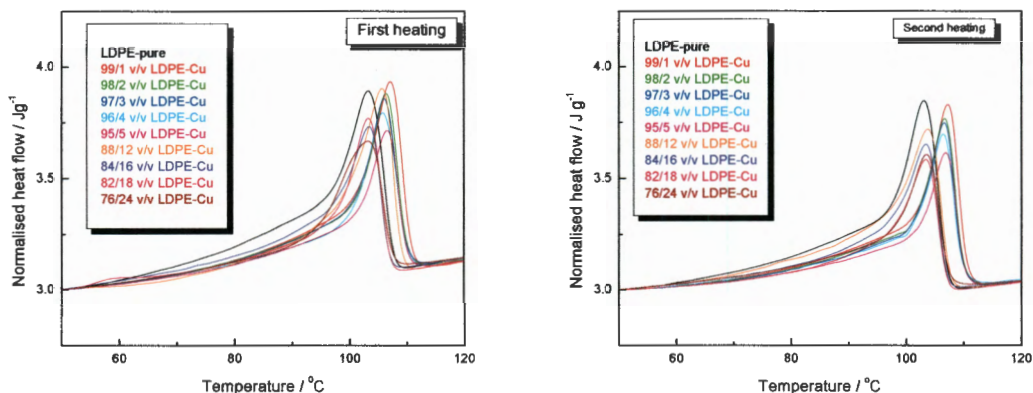


Figure 3.3 DSC heating curves of LDPE and its copper composites

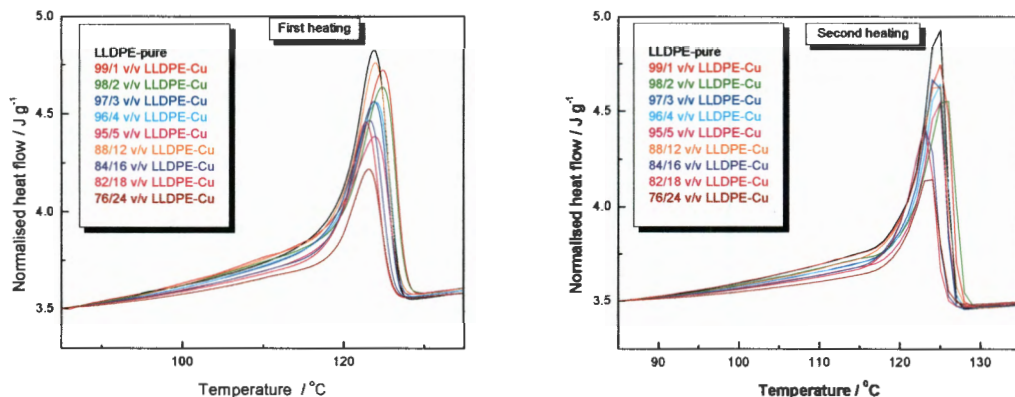


Figure 3.4 DSC heating curves of LLDPE and its copper composites

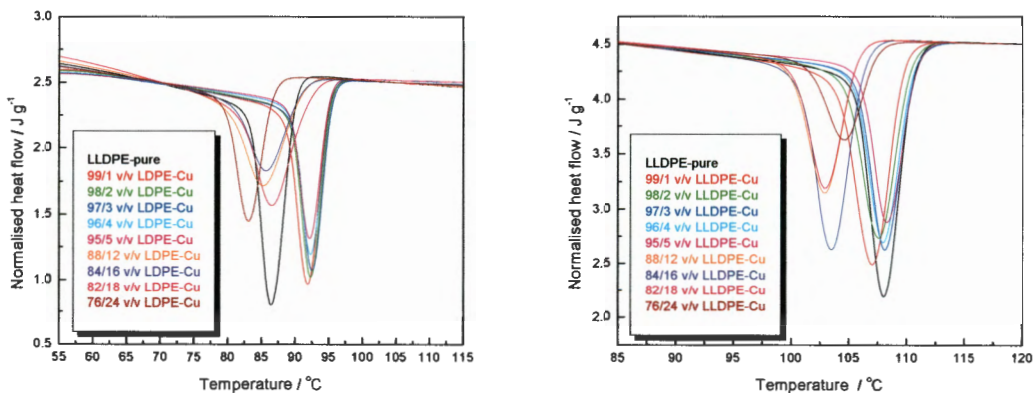


Figure 3.5 DSC cooling curves of LDPE, LLDPE and their copper composites

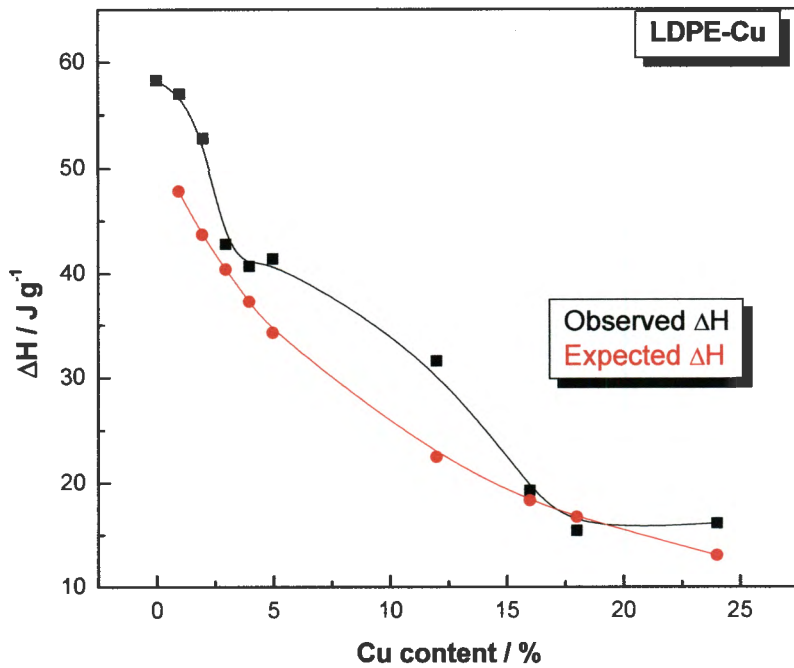


Figure 3.6 Experimental and theoretically expected melting enthalpies as function of Cu content in the LDPE composites

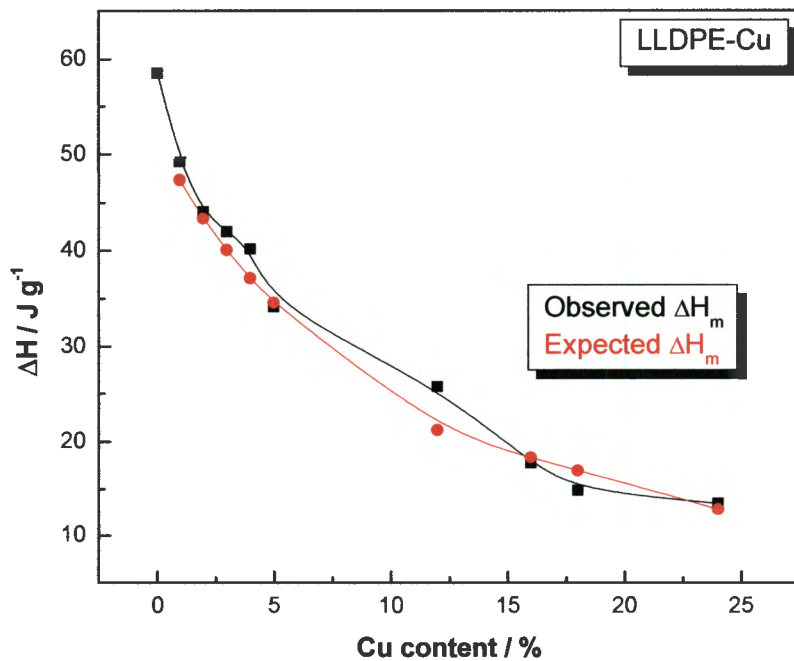


Figure 3.7 Experimental and theoretically expected melting enthalpies as function of Cu content in the LLDPE composites

3.3.2 Thermogravimetric analysis (TGA)

The TGA curves for LDPE, LLDPE and their copper composites are shown in Figure 3.8, and the onset temperatures of decomposition are summarized in Table 3.4. There seems to be a general decrease in thermal stability with increasing copper content in both LDPE and LLDPE. There are, however, a few exceptions to the general trend, and these may be because (i) the thermographic analyzer did not have the same calibration parameters during the analyses of the different samples, or because (ii) the copper distribution differed from sample to sample. It was, however, not possible to repeat these analyses because of serious problems with the instrument. A possible explanation for the decrease in thermal stability is that, since copper has a relatively high heat capacity, most of the heat is absorbed by the copper, which makes it a very localized source of heat energy. Thermal decomposition of the PE matrix is then initiated at a lower temperature.

Table 3.4 Onset temperatures of decomposition of LDPE, LLDPE and their copper composites

Vol.% Cu	Onset temperature / °C	
	LDPE	LLDPE
0	392.0	489.0
1	478.1	428.0
3	404.9	481.6
4	476.8	432.8
5	420.0	491.7
16	419.5	422.1
18	415.1	423.2
24	416.8	427.1

Table 3.5 compares the % residue of the different samples with the wt.% copper initially mixed with the polyethylenes. Although there is a good correlation between the values, there are some differences, especially at higher Cu contents. This shows that the copper did not homogeneously mix with the matrix in all cases.

Table 3.5 Comparison of wt.% copper mixed into PE with wt.% residue at the end of the TGA

Vol.% Cu	LDPE		LLDPE	
	Wt.% residue	Wt.% Cu in PE	Wt.% residue	Wt.% Cu in PE
1	8.9	8.9	8.3	8.9
3	22.3	23.1	22.5	23.1
4	27.5	28.7	28.6	28.6
16	65.4	65.0	63.2	65.0
18	66.7	68.1	68.1	68.1
24	79.5	82.0	75.3	82.0

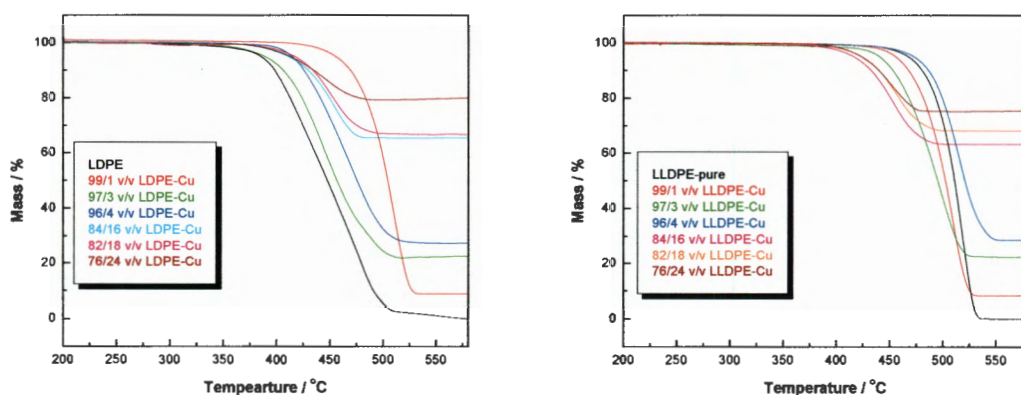


Figure 3.8 TGA curves of LDPE, LLDPE and their copper composites

3.4 Mechanical properties

Figures 3.9 and 3.10 show typical stress-strain curves for LDPE, LLDPE and their copper composites. A possible reason for the differences between replicate tests is the non-homogeneous distribution of copper powder in the polymer matrices (see Figure 3.1).

Tables 3.6 and 3.7 summarizes the tensile properties of LDPE, LLDPE and their copper composites. The dependence of these values on the copper content in the composites is illustrated in Figures 3.6 – 3.8.

Table 3.6 Mechanical properties of LDPE-Cu composites

Vol.% Cu	$\epsilon_b \pm s\epsilon_b / \%$	$\sigma_b \pm s\sigma_b / \text{MPa}$	$E \pm sE / \text{MPa}$
0	181.0 ± 40.0	9.4 ± 0.4	94.8 ± 3.1
2	157.0 ± 34.0	8.2 ± 0.2	95.9 ± 1.6
3	146.0 ± 5.9	7.7 ± 0.3	94.0 ± 1.9
4	158.0 ± 18.0	8.3 ± 0.1	98.0 ± 2.7
5	73.0 ± 6.0	7.9 ± 0.1	99.4 ± 4
12	43.0 ± 1.2	8.6 ± 0.4	120.0 ± 1.1
16	36.5 ± 1.4	8.7 ± 0.3	123.0 ± 6.3
18	21.9 ± 0.7	9.0 ± 0.5	140.0 ± 7.0

ϵ_b – elongation at break, σ_b – stress at break, E – tensile modulus

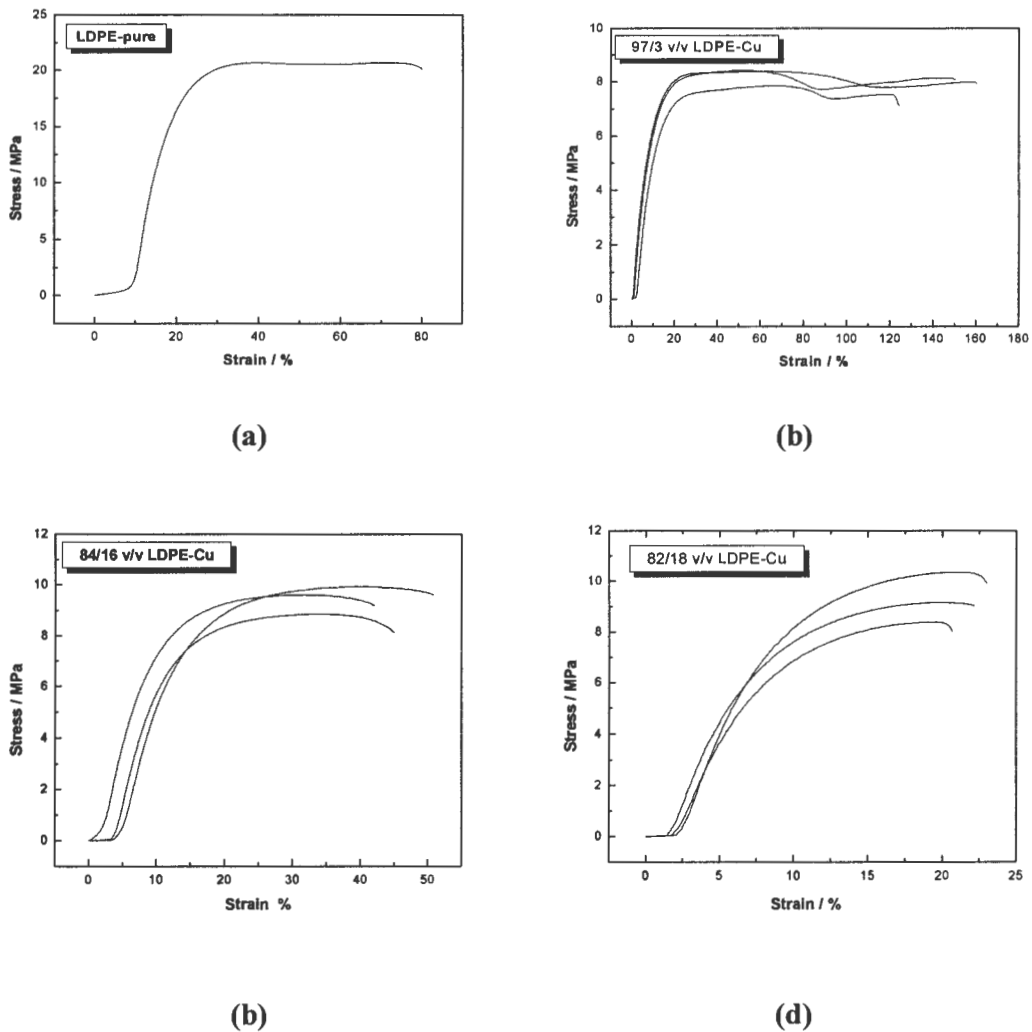
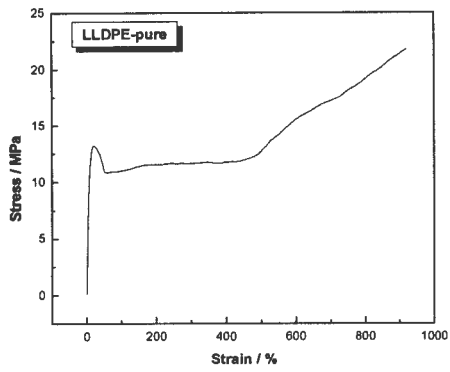
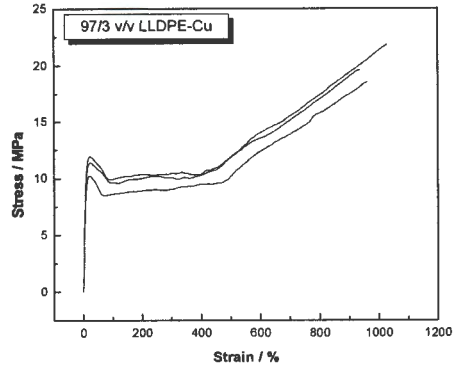


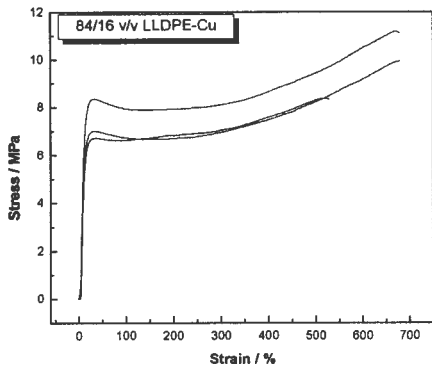
Figure 3.9 Stress-strain curves for pure LDPE and its copper composites



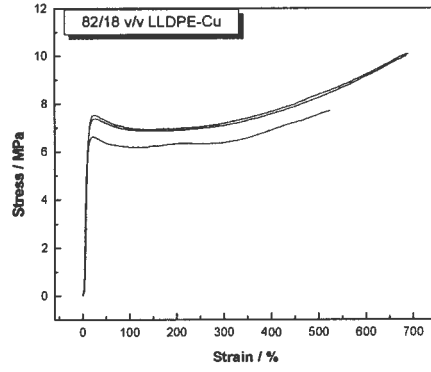
(a)



(b)



(b)



(d)

Figure 3.10 Stress-strain curves for pure LLDPE and its copper composites

Table 3.7 Mechanical properties of LLDPE-Cu composites

Vol.% Cu	$\epsilon_b \pm s\epsilon_b / \%$	$\sigma_b \pm s\sigma_b / \text{MPa}$	$E \pm sE / \text{MPa}$
0	1219.0 \pm 58.0	27.1 \pm 0.7	118.4 \pm 4.7
2	1119.0 \pm 16.0	21.5 \pm 0.2	104 \pm 3.6
3	1084.0 \pm 23.4	20.4 \pm 0.7	114 \pm 1.5
4	851.0 \pm 22.7	17.9 \pm 0.5	114 \pm 5.0
5	863.4 \pm 80.0	17.4 \pm 2.0	122 \pm 6.0
12	685.0 \pm 31.0	12.8 \pm 1.1	165 \pm 1.5
16	713.0 \pm 25.0	13.0 \pm 0.3	142 \pm 3.4
18	636.0 \pm 13.4	11.0 \pm 0.5	153 \pm 7.5

ϵ_b – elongation at break, σ_b – stress at break, E – tensile modulus

For LDPE the elongation and stress at break slightly decrease with increasing copper content (Figures 3.11 and 3.12), while the decrease in the case of LLDPE is much more significant. Pure LLDPE has a high value of elongation as well as stress at break compared to LDPE, probably because of the difference in branching between the two polymers. Adding filler to the polymer matrix results in a decrease in both elongation and stress at break. LLDPE has a high value of elongation at break, because when force is applied, the polymer chains have enough space and time to orientate, which is the result of the chemical structure of LLDPE. Immediately when the chains are oriented, they start to form orientation crystallinity, which evokes an increase in the strength of a sample. Adding filler to the polymer matrix reduces chain mobility, giving rise to a rapidly decreasing elongation at break. Generally, a decrease in elongation at break with an increase in filler content is observed. A few models have been suggested for this behaviour. The most well known is Nielsen's model [94]. This model is valid if particles have a spherical shape assuming adhesion between the phases. Many fillers do not fulfill these conditions, as seen in Figure 3.1 where it is clear that the filler particles do not have a uniform size distribution. These factors probably contribute significantly to a dramatic decrease in elongation at break. At medium filler content, a number of stress concentrating sites are formed, and they are not close to each other. In some sites the inhomogeneities may lead to a favourable situation for fast crack growth. A general decrease in stress at break is also observed in the composites. This behaviour is probably the result of poor interaction between the polymer and filler. For both LDPE and LLDPE the largest decrease is observed up to 5 vol.% copper, whereafter the influence of copper on these properties is less dramatic. This indicates that the presence of the filler in the matrix hinders

the sample to deform due to polymer chain mobility, which makes it difficult for the segments of polymer materials to easily slip past each other.

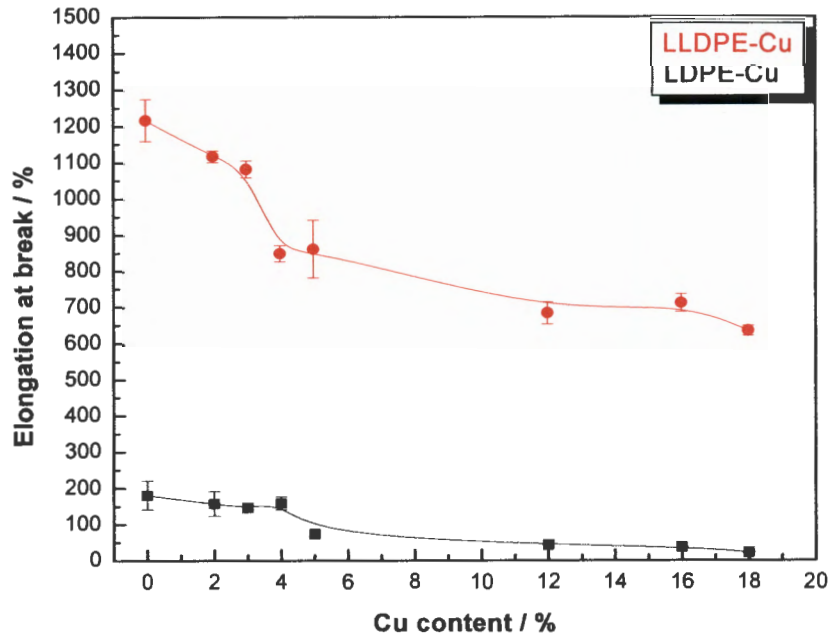


Figure 3.11 Elongation at break as function of copper content in the composites

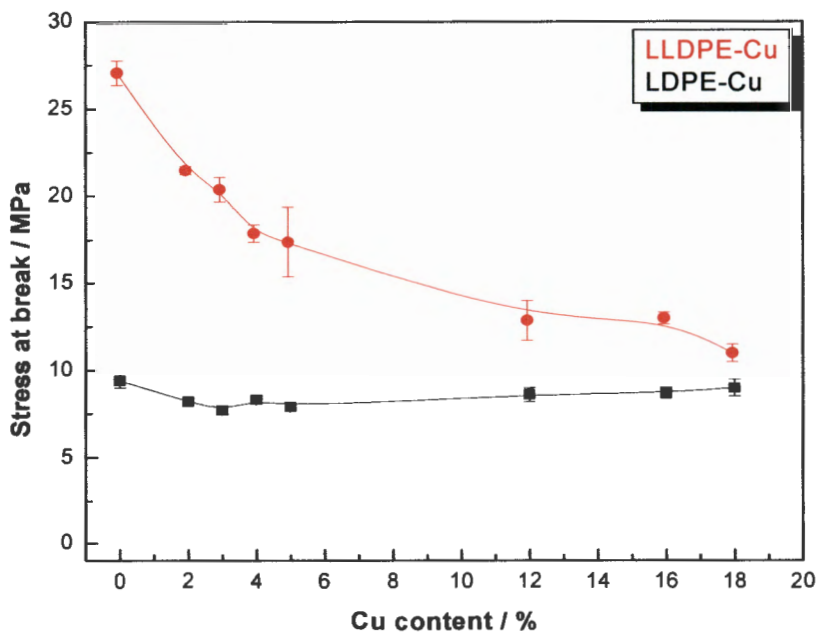


Figure 3.12 Stress at break as function of copper content in the composites

The dependence of Young's modulus of the composites on the volume percentage of filler is shown in Figure 3.13. Young's moduli of LLDPE and its composites have slightly higher values than those of LDPE and its composites, because LLDPE is more crystalline and therefore more stiff than LDPE. These values strongly decrease from the values for both pure LDPE and LLDPE to those of their composites containing 2 vol.% copper, after which the moduli slightly increase with increasing copper content. The initial decrease is probably the result of the weak interaction between PE and copper, giving rise to more freedom of chain movement, despite the higher than expected crystallinity (see discussion of DSC results). The size and distribution of filler particles also play a significant role, since the filler is much stiffer than the polymer matrices and the stiffness increases with increasing filler content. This behaviour was also observed in previous studies where investigations showed that mechanical properties are influenced by the reinforcing effect of the metal fillers [73]. The extent depends on the filler surface area, as indicated by an increase in Young's modulus, and a decrease in both elongation and stress at break.

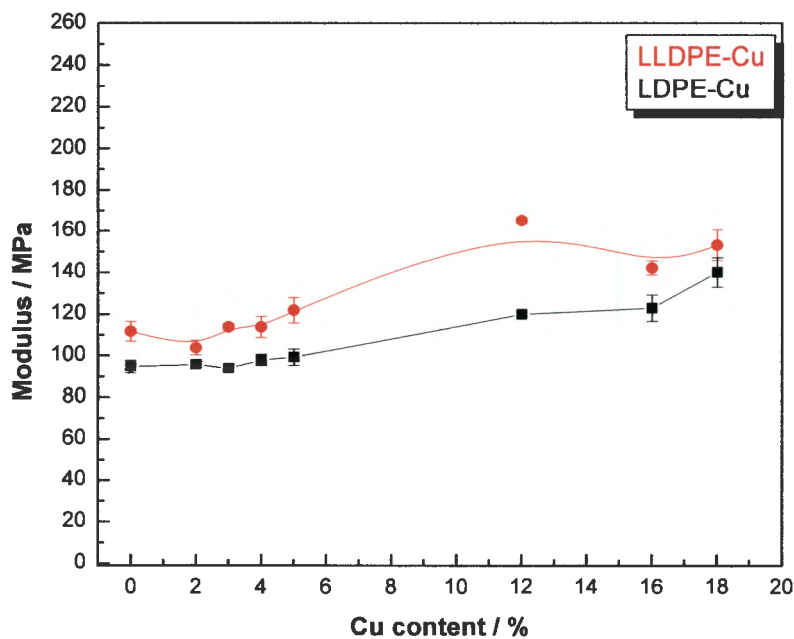


Figure 3.13 Young's modulus as function of copper content in the composites

3.5 Thermal and electrical conductivity

The values of the thermal and electrical conductivity of LDPE and LLDPE and their copper composites are presented in Table 3.7. The dependence of the thermal conductivity on copper content is shown in Figure 3.14. It is clear that the thermal conductivities of the composites are higher than that of the pure polyethylene matrix for both LDPE and LLDPE. A linear increase in thermal conductivity is observed with an increase in filler content. The reason is that more conductive paths are created as a consequence of the higher content of copper powder particles (see photos in section 3.1).

Table 3.7 Thermal conductivity and specific resistivity of LDPE, LLDPE and their copper composites

SAMPLES	Thermal conductivity / $\text{W m}^{-1} \text{K}^{-1}$	Specific resistivity / $\Omega\cdot\text{cm}$
LDPE	0.31	13.79
93/7 w/w LDPE-Cu	0.35	13.18
88/12 w/w LDPE-Cu	0.43	12.58
86/14 w/w LDPE-Cu	0.51	12.49
84/16 w/w LDPE-Cu	0.63	12.32
82/18 w/w LDPE-Cu	0.65	11.39
78/22 w/w LDPE-Cu	0.68	8.97
76/24 w/w LDPE-Cu	0.72	8.91
LLDPE	0.36	13.91
93/7 w/w LLDPE-Cu	0.39	13.61
88/12 w/w LLDPE-Cu	0.55	13.30
86/14 w/w LLDPE-Cu	0.57	13.11
84/16 w/w LLDPE-Cu	0.59	12.08
82/18 w/w LLDPE-Cu	0.68	11.32
78/22 w/w LLDPE-Cu	0.71	8.95
76/24 w/w LLDPE-Cu	0.76	8.53

The thermal conductivity is higher in the LLDPE matrix than in the LDPE matrix for all copper contents. The reason is probably that more conductive paths are created as a consequence of higher agglomeration of particles [72]. Since the Cu particles are restricted to the amorphous parts of a polymer, and since LLDPE has lower amorphous content, it is quite possible that there will be more agglomeration of particles in the LLDPE matrix.

From Figure 3.15 it can be seen that the electrical conductivity of polyethylene-copper composites increases with increasing copper content in the composite for both LDPE and LLDPE. From this graph the percolation concentration may be determined. At this concentration at least one cluster of particles is formed in the polymeric matrix. This cluster penetrates throughout the sample, while the particles in the cluster are in close contact and represents a conductive path for the movement of electrons throughout the sample. The percolation point has been arbitrarily identified as the inflexion point in an empirical fitting curve. The percolation concentrations are almost the same for both LDPE and LLDPE composites, and the value was determined to be 18.7 vol.%. According to Lux [100] the percolation concentration strongly depends on the shape of the particles, but should not depend on their size. Figure 3.15 shows that the electrical conductivities of LDPE-Cu composites are generally higher than those of LLDPE-Cu composites. This is probably the result of the more amorphous nature of LDPE, which allows higher mobility of the copper particles.

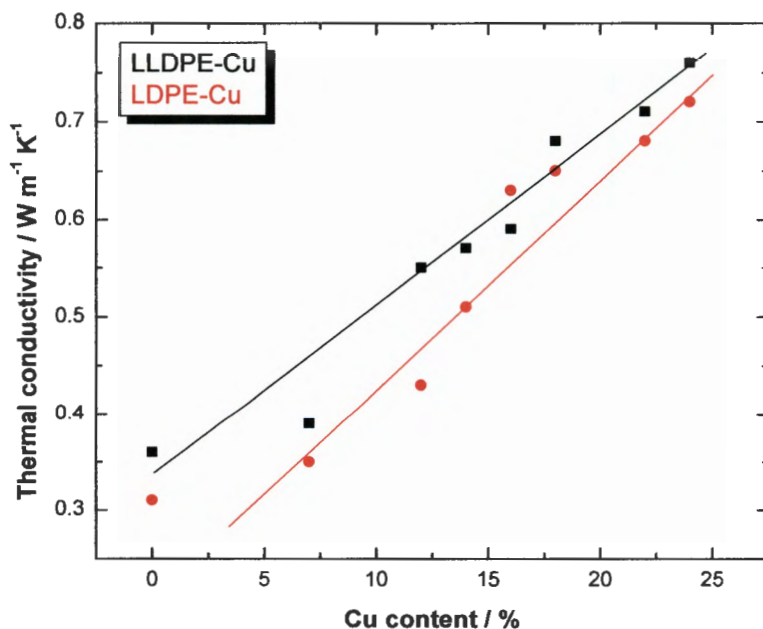


Figure 3.14 Thermal conductivity of the composites as function of copper content

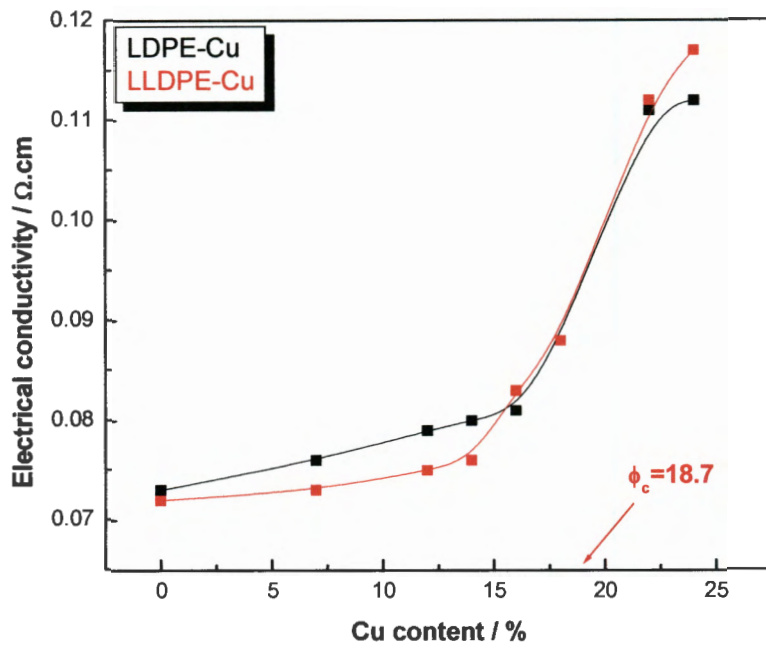


Figure 3.15 Electrical conductivity of the composites as function of copper content

CHAPTER FOUR

CONCLUSIONS

The aim of this study was to prepare LDPE-Cu and LLDPE-Cu composites containing different amount of copper, and to determine the morphology, surface free energy, thermal and mechanical properties, as well as thermal and electrical conductivities of the samples. These properties were compared as function of copper content, and its was attempted to explain the observations in terms of the morphologies of the composite samples.

The copper powder particle distributions were found to be relatively uniform at both low and high copper contents. There were, however, large variations in copper particle size distributions. There was cluster formation of copper particles at higher Cu contents, as well as the formation of percolation paths of copper in the PE matrices.

The surface free energy results show an increase in the total surface free energy and its disperse part, but a decrease in the polar part of the surface free energy for the Cu-PE composites in comparison with pure PE. The respective increase and decrease of values is relatively strong after addition of low amounts of copper, whereafter the values slightly increase with increasing copper content.

There was an initial increase, followed by a decrease in melting temperature of LDPE with increasing copper content. This is the result of changing lamellar thickness, which is due to additional crystallization in the presence of copper. It may be explained through LDPE chains in the amorphous phase crystallizing epitaxially on the copper particle surfaces. When the observed enthalpy was compared with the expected enthalpy, a higher enthalpy was observed in the presence of low copper contents. This indicated higher crystallinity, which supports the explanation above. For LLDPE the melting temperatures did not change appreciably. This indicates that lamellar thickness was not influenced by the presence of copper in the polymer matrix. The reason for this is probably that LLDPE has a relatively high crystallinity, and there is not a major amorphous part in which the copper particles can be accommodated. The copper particles therefore probable locate themselves in the interlamellar spaces, which leaves very little room for additional crystallization. Comparison of the observed and expected enthalpies also showed that there was very little increase in total crystallinity.

The TGA results show that there was a general decrease in thermal stability with increasing copper content in both LDPE and LLDPE. A possible explanation for this is that, since copper has a relatively high heat capacity, most of the heat is absorbed by the copper, which makes it a very localized source of heat energy. Thermal decomposition of the PE matrix is then initiated at a lower temperature.

For LDPE the elongation and stress at break slightly decreased with increasing copper content, while the decrease in the case of LLDPE was much more significant. Adding filler to the polymer matrix reduced chain mobility, giving rise to a rapidly decreasing elongation at break. The decrease in stress at break probably is the result of poor interaction between the polymer and filler. Young's moduli of LLDPE and its composites had slightly higher values than those of LDPE and its composites, because LLDPE is more crystalline and therefore more stiff than LDPE. These values strongly decreased from the values for both pure LDPE and LLDPE to those of their composites containing 2 vol.% copper, after which the moduli slightly increased with increasing copper content. The initial decrease is probably the result of the weak interaction between PE and copper, giving rise to more freedom of chain movement, despite the higher than expected crystallinity. The size and distribution of filler particles also play a significant role, since the filler is much stiffer than the polymer matrices and the stiffness increases with increasing filler content.

The thermal conductivities of the composites were higher than that of the pure polyethylene matrix for both LDPE and LLDPE. A linear increase in thermal conductivity was observed with an increase in filler content. The reason is that more conductive paths are created as a consequence of the higher content of copper powder particles. The electrical conductivity of polyethylene-copper composites increased with increasing copper content in the composite for both LDPE and LLDPE. From these results the percolation concentration was determined as 18.7 vol.% copper for both polymers.

REFERENCES

1. Prasad NSK in *Hardy composites publication and information directorate (CSIR)*, New Delhi (1992) 5
2. Seyman RD and Cecaraha JR, *Structure Property Relationship in Polymers*, Plenum Press, New York (1984) 122
3. Nielson LE in *mechanical properties of polymers and composites*, Dekker; New York (1974).
4. Parrot N in *Fiber reinforced materials technology*, Van Nostrand-Reinhold, Van Nostand-Reinhold, New York (1969)
5. G Babu Rao, *PhD thesis*, 2002, Department of Polymer Science and Technology, Sri Krishnadevaraya University, India
6. Schruben DL, *Polymer Engineering Science*, 29(1989) 420
7. Bueche F, *Journal of Apply Physics*, 43 (1972) 4837
8. Sherman RD, Middleman LM, and Jacobs SM, *Elsevier Polymer Engineering Science*, 23 (1983) 36
9. Nagata K, Iwabuki H, Nigo H, *Composite Interference*, 6 (1999) 484
10. Yu-chuan L, and Kun-Cheng C, *Synthetic Metals*, 139 (2003) 277
11. Wiriya T, Richard Spontak J and Maurice Balik C, *Polymer Journal*, 43 (2002) 2279
12. Miyasaka K, Watanabe K, Jojima E, Aida H, Sumita M and Ishikawa K, *Journal of Materials Science*, 17 (1982) 610
13. Kirkpatrick S, *Review Modern Physics* 45 (1973) 574
14. Abeles B, Pinch HL and Gittleman JI, *Physics Review Letters*, 35 (1975) 247
15. Wang YS, Ogurkis MA and Lindt JT, *Polymer Composites*, 7 (1986) 349
16. Cespedes F, Martinez Fabregas E and Alegret S, *Trac-Terends Anal Chem*, 15 (1996) 296
17. Huiru Gu, Xiaodi S, and Kian Ping L, *Chemical Physics letters*, 388 (2004) 483
18. Zhao, Wenxue Y, Xiujuan He, and Xinfang C, *Materials Letters*, 57 (2003) 3082
19. Yu-chuan and Bing-Joe H, *Thin Solid Films*, 360 (2000) 1
20. Feller JF, Langevin D and Marais S, 144 (2004) 81
21. Dilhan Kalyon M, Elvan B, Rahmi Y, Bahadir K, and Shawn W, *Polymer Engineering and Science*, 42 (2002) 609
22. Yazici R, Karuv B, Garrow J, Birinci E and Kalyon D M, *SPE ANTEC Technical Papers*, 45 (1999) 1551

23. Zallen R, *The Physics of Amorphous Solids* (J. Wiley and Sons, New York, 1983)
24. Mamunya Ye P, Davydenko VV, Pissis P and Lebedev EV, *European Polymer Journal*, 38 (2002)1887
25. Stauffer D, *Introduction to percolation theory*, Taylor and Francis, London (1985)
26. Katz HS and Milewski JV, Editors, *Handbook of fillers and reinforcements for plastics*, Van Nostrand Reinhold, New York (1978)
27. Mamunya EP, Davydenko VV and Lebedev EV, *Kompoz Polym Mater*, 50 (1991) 37
28. McGeary RK, *Journal Am Ceram Soc*, 44 (1961) 513
29. Scher H and Zallen, *Journal Chemical Physics*, 53 (1970) 3759
30. Lux F, *Journal Material Science*, 28 (1993) 285
31. Efros AL and Shklovskii BI, *Phys Stat Sol B*, 76 (1976) 475
32. Mamunya EP, Davydenko VV and Lebedev EV, *Composite Interference*, 4 (1997)169
33. Wessling B, *Synthetic Metals*, 45 (1991)119
34. Bhattacharya SK, Editor, *Metal-filled polymers (properties and applications)*, Marcel Dekker, New-York (1986)
35. Kusy RP and Corneliussen RD, *Polymer Engineering Science*, 15 (1975) 1
36. Mamunya Ye P, *Journal Macromolecule Science of Physics B*, 38 (1971) 614
37. Tchoudakov R, Breuer O, Narkis M and Siegmann A, *Polymer Engineering Science*, 36 (1996) 1336
38. Feller JF, Linossier I and Grohens Y, *Materials Letters*, 57 (2002) 64
39. Novák I, Krupa I and Chodák I, *European Polymer Journal*, 39 (2003) 585
40. Novák I, Krupa I, Chodák I, *Synthetic Metals*, 131 (2002) 93
41. Lei Yang and Dale L Schruben, *Polymer Engineering and Science*, 34 (1994) 1109
42. Zhin-Min D, Yi-He Z and Tjong S-C, *Synthetic Metals*, 146 (2004) 79
43. DM Yu and Wu JS, *Composite Sciences and Technological Science*, 60 (2000) 499
44. Psarras GC, Manolakaki E and Tsangarris GM, *Composites A*, 33 (2001) 375
45. Dilhan Kaylon M and Evan B, *Society of Plastics Engineers ANTEC Technical papers*, 2 (2002) 1716
46. Bigg DM, in *Metal Filled Polymers*, S Bhattacharya, ed., 165-226, Marcel Dekker, New York (1996)
47. Bigg DM, *Advanced Polymer Technology*, 3/4, 255 (1984)
48. Margolis JM, *"Conductive Polymers and Plastics"*, Chapman & Hall, New York (1989)
49. Delmonte J, *Metal/Polymer Composites*, Van Nostrand, New York (1990)
50. Narkis M, Srivastava S, Tchoudako R and Breuer O, *Synthetic Metals* 113, 29-34 (2000)

51. Cheah K, Forsyth M and Simon G, *Synthetic Metals*, 102 (1999) 1232
52. Mamunya Ye P, Zois H, Apekis L and Lebedev EV, *Powder Technology*, 140 (2004) 49
53. Das NC, Chaki T K and Khastgir D, *Carbon*, 40 (2002) 807
54. Baltacolleja FJ, Ezquetva TA and Rueda D R, *Journal Material Res* 3 (1984) 165
55. Jana PB, Chaudhuri S, Pal AK and De SK, *Polymer Engineering Science*, 32 (1992) 448
56. Das NC, Chaki TK, Khastgir D and Chakraborty A, *Polymer Composite*, 8 6 (2000) 395
57. Shinn-Shyong T and Fa-Yen C, *Materials Science and Engineering A*, 302 (2001) 258
58. Philip Michael C, Nannaji S and Rabinowicz E, *Wear* 127 (1988) 15
59. Vilčáková J, Paligová M, Omastová M, Sába P and Quadrat O, *Synthetic Metals*, 146 (2004) 121
60. Kuljanin J, Vučković M, Čomor MI, Bibić N, Djoković V, Nedeljković JM, *European Polymer Journal* 38 (2002) 1659
61. Weidenfeller B, Höfer M and Frank Schilling R, *Composite Part A: Applied Science and Manufacturing*, 35 (2004) 423
62. de Araujo FFT and Rosenberg H M, *Journal of Physics D: Applied Physics.*, 9 (1276)
63. Do Kim Y, Nang Lyeom O, Sung-Tag O and In-Hyung M, *Materials Letters*, 51 (2001) 420
64. Koráb J, Štefánik P, Kavecký Š, Šebo P and Korb G, *Composite Part A: Applied Science and Manufacturing*, 33 (2002) 577
65. Brito Z and Sánchez G, *Composite Structures*, 48 (2000) 79
66. James Gaier R, Yoder Vandenberg Y, Berkebile S, Stueben H and Balagadde F, *Carbon*, 41 (2003) 2187
67. Piraux L, Nysten B and Haquenne A., The temperature variation of the thermal conductivity of benzene-derived carbon fibers, *Solid State Commun*, 50 8 (1984) 697
68. Dresselhaus MS and Dresselhaus G, Intercalation compounds of graphite, *Advanced Physics*, 30 2 (1981)139
69. McDaniels DL, Baker KW and Ellis DL, Graphite fiber/copper matrix composites for space power heat pipe fin applications, Inc: Proceedings 8th Symposium space nuclear power systems (1991) 313
70. Suzhu Y, Hing P and Xiao H, *Composite Part A: Applied Science and Manufacturing*, 33 (2002) 289
71. Agari Y, Ueda A and Gagai S, *Journal of Applied Polymer Science*, 42 (1991) 1665
72. Krupa I and Chodak I, *European Polymer Journal*, 37 (2001) 2159
73. Bigg DB, *Advanced Polymer Science*, 119 (1995)1

74. Sundstrom DW, Lee YD, *Journal of Applied Polymer Science*, 16 (1972) 3159
75. Weidenfeller B, Höfer M and Frank Schilling R, *Composite Part A: Applied Science and Manufacturing*, 35 (2004) 423
76. Hashin Z and Shtrikman A, variational A, approach to the theory of the effect magnetic permeability of multiphase materials, *Journal of Apply Physics*, 33 (1962) 3125
77. Baré W, Albano C, Reyes J and Domínguez N, *Surface and Coatings Technology*, 158-159 (2002) 404
78. Chodak I, Krupa I, *Journal of Materials Science Letters*, 18 (1999) 1457
79. Fan L, Dang Z, Ce-Wen N and Ming L, *Electrochimica Acta*, 48 (2002) 205
80. Paul Bloom D, Baikerikar KG, James W Anderegg and Valerie V Sheares, *Materials Science and Engineering A*, 360 (2003) 46
81. Vardavoulias M, Jouanny-Tresy C and Jeandin M, *Wear* 165 (1993) 141
82. Durand JM, Vardavoulias M and Jeandin M, *Wear*, 181-183 (1995) 833
83. Anderson Brian C, Bloom Paul D, Baikerikar KG, Valerie V Sheares and Surya Mallapragada K, *Biomaterials*, 23 (2002) 1761
84. Seong Su K, Chang P D and Lee D G, *Composite Structures*, 66 (2004) 359
85. Bloom Paul D, Baikerikar KG, Joshua Otaigbe U and Valerie Sheares V, *Materials Science and Engineering A*, 294-296 (2000)156
86. Katz HS, Milewski JV (Eds.), *Handbook of fillers for Plastics*, Van Nostrand Reinhold, New York, 1987, 34
87. Weick BL and Bhushan B, *Wear* 202 (1996) 17
88. Cartz, L., *Nondestructive Testing*, ASM International, *Materials Parks*, OH (1995) 135
89. Gao Jintang, *Wear*, 245 (2000) 100
90. Marzouk PK Turunen, Marjamäki P, Paajanen M, Lahtinen J and Jorma Kivilahti K, *Microelectronics Reliability*, 44 (2004) 993
91. Schultz J, *Polymer Materials Science* (Prentice-Hall, Englewood Cliffs, NJ, 1974) 158
92. Toledo-Crow R, Yang PC, Chen Y, and Vaez-Iravani M, *Applied Physics Letters*. 60, (1992) 2957
93. Williamson RL and Miles MJ, *Journal Vac Sci Technol B*, 14 (2) Mar/Arp 1996
94. Nielsen R, *Mechanical Properties of Polymers and Composites 2*, New York: Marcel Dekker; 1974
95. Bujard P, Munk K and Kuehnlein G In: Tong TW, editor, *Thermal Conductivity 22* Lancaster, Basel: Technomic Publishing; (1994) 711
96. Jančár J, *Plasty a Kaučuk* 27 (1990) 289 [in Czech]

97. Agari Y and Uno T, *Journal of Applied Polymer Science*, 32 (1986) 5705
98. Agari Y, Ueda A and Nagai ST, *Journal of Applied Polymer Science*, 49 (1993) 1625
99. Wunderlich B, *Macromolecular physics II*. New York: Academic Press; 1973
100. Lux F, *Journal of Material Science*, 18 (1999)1457

ACKNOWLEDGEMENTS

- I would like to express my sincere gratitude to my supervisor, Prof AS Luyt, for being patient, helping, guiding me throughout the project and in assisting me with the interpretation of results.
- I want to thank Dr H Krump, Dr B Guduri and Dr V Djoković for their inputs in the interpretation of the results.
- I also like to thank Physics Department people with their inputs (Dr Tchoulachokonte M & Dr Dejene F)
- Many thanks to my fellow research team for their contribution in this project during the start and throughout the project.
- The work was supported financially by the NRF
- I would also like to thank my friends and family for their moral support throughout the project, Soso Ngubeni (mentor), Seunkie Sebata and Family, Mapula Motsoeneng*, Thabo Molefi , Dineo Ntatsane and family, Papiki Ngubeni, Tsotetsi Tsietsi Tsika, Maduna Sabata, Puseletso Mofokeng, Moeketsi Matebesi, Mphutlane wa Bofelo, Mondi Nkosi, Mbhekezele Maduna, Enerst Neshunzi and Family, Sam Nhlapo Kgopolo Noka, Siphon Mchachu, Lenyona Mabuya, Salman letlatsa and Family, Bende Mark, Neo Magage, Senokoane Seadimo, Itumeleng Taiwe, Teboho Sithole, Nkosingiphile Shabalala, Makgadiete Salemane, Hato Mamale, Mamookho Malunka, Sebenzile Mpanza, Tumelo Sekhoto, Mathabo Sekhoto, Tshediso Fantisi Papi, Mamokete Chabedi,,Mamokete Tau, Thabang and Paledi Legwabe, Daddy and Pheello Potsane, Larcy Tsolo and Family, Dumisane Tshabalala, George Tshabalala,Thami Kati,Faeza Housein, Palesa Matsoso, Search Mnguni & Family, Makgotso Madimabe and my brother & sister (Tefo & Ditsietsi), Ausi Nosipho Mthata and family, Dorine Dikobe,Percy Hlangothi, Martin Ntwaeaborwa, Boyz Bafana ka Phutha. Sabata Chabedi and Family, Moipone Mokoena and little brothers (Neo, Teboho and Itumeleng), Moloi Joyce Mbokeleng, Joel Motloun,
- Thanks to my mother Mzondase Kheswa and my late grand mother Mmapheello Anah Lehula who by example taught me the values of life for which is strive to live by.
- Finally all thanks are due to the most gracious, most merciful the Almighty God through whose will everything happens.